Summer 8-2010

Relativistic Studies of the Charmonium and Bottomonium Systems Using the Sucher Equation

Charles Martin Werneth
University of Southern Mississippi

The University of Southern Mississippi

RELATIVISTIC STUDIES OF THE CHARMONIUM AND BOTTOMONIUM SYSTEMS USING THE SUCHER EQUATION

by

Charles Martin Werneth

Abstract of a Dissertation
Submitted to the Graduate School
of The University of Southern Mississippi
in Partial Fulfillment of the Requirements
for the Degree of Doctor of Philosophy

August 2010

ABSTRACT

RELATIVISTIC STUDIES OF THE
CHARMONIUM AND BOTTOMONIUM SYSTEMS
USING THE SUCHER EQUATION

by Charles Martin Werneth
August 2010

In this dissertation, bound states of quarks and anti-quarks (mesons) are studied with a relativistic equation known as the Sucher equation. Prior to the work in this dissertation, the Sucher equation had never been used for meson mass spectra. Furthermore, a full angular momentum analysis of the Sucher equation has never been studied. The Sucher equation is a relativistic equation with positive energy projectors imposed on the interaction. Since spin is inherent to the equation, the Sucher equation is equivalent to a relativistic Schrödinger equation with a spin-dependent effective potential. Through a complete general angular momentum analysis of the equation, we found that different angular momenta can couple through the effective potential without explicitly using tensor interaction. Next we expanded the wave functions in a complete set of basis functions and converted the Sucher equation into a matrix eigenvalue equation. As a practical application, we fit to the low lying states of the bottomonium and charmonium systems with the minimal number of input parameters, and we were able to predict the remaining spectra. We find that the the Sucher equation may be used for charmonium and bottomonium spectra. However, the spin dependent interactions inherent to the Sucher equation do not produce adequate energy level splitting between singlet and triplet states.

The University of Southern Mississippi

RELATIVISTIC STUDIES OF THE CHARMONIUM AND BOTTOMONIUM SYSTEMS USING THE SUCHER EQUATION

by

Charles Martin Werneth

A Dissertation
Submitted to the Graduate School
of The University of Southern Mississippi
in Partial Fulfillment of the Requirements
for the Degree of Doctor of Philosophy

Approved:

Dr. Khin Maung Maung

Director

Dr. Lawrence Mead

Dr. Christopher Winstead

Dr. Sungwook Lee

Dr. John Norbury

Dr. Susan A. Siltanen

Dean of the Graduate School

August 2010

ACKNOWLEDGMENTS

There are many people who have helped me throughout my educational studies. Foremost, I must thank my family for their constant support and encouragement. I thank my father for encouraging me to study science and mathematics at an early age and for his belief in my ability. I also thank him for helping me with supplies and transportation while I studied. I thank Patti Werneth for her endless support, encouragement, guidance, and good times. I thank my mother and Jerry Wells for always supporting me in whatever I chose to do. You have been a constant source of inspiration for me. I thank my sister, brother-in-law, and nephews for their support of me throughout my studies and for all of the fun times. I also thank Jennifer Wells for her support. I am very lucky indeed to have such a family.

I thank Dr. Khin Maung Maung for his support and encouragement. I appreciate all of the time you spent and the late nights you worked to help me. I also thank you for providing me with a research topic I really enjoyed. Thank you for making the learning process enjoyable and exciting. Most of all, thank you for your friendship and for believing in me. I also thank your family for treating me as one of their own.

I thank Mallika Dhar for her interesting conversations, friendship, and help with many areas of my research. I thank my committee members Drs. John Norbury, Lawrence Mead, Sung Lee, and Chris Winstead for their insight and useful suggestions. In particular, I would like to thank Dr. John Norbury for working so hard to help get the results of our work published. I would like to thank Drs. Steve Blattnig, Martha Clowdsley, Robert Singleterry, Francis Badavi, Ryan Norman, and Anne Adamczyk at NASA Langley for all of their help and for making me feel welcome. I also thank Chris Pike for his friendship and encouragement.

I would be remiss if I did not thank those instructors who encouraged me at the earlier stages of my education: Carol Lee, Linda France, Barbara Taylor, Mona Lisa Blackburn, and Dr. Jason Pugh. I am truly grateful to you and to everyone else who have helped me.

Finally, this dissertation is dedicated to the memory of my gradfather, Al Scivicque, who passed away while I was writting this document. I have always admired your love for your family, dedication to your work, and wonderful sense of humor. You will be missed.

TABLE OF CONTENTS

LIST OF ILLUSTRATIONS

Figure

LIST OF TABLES

Table

LIST OF ABBREVIATIONS

QCD - Quantum Chromodynamics
QED - Quantum Electrodynamics
OGE - One Gluon Exchange

NOTATION AND GLOSSARY

General Usage and Terminology

In this dissertation all vectors are indicated in bold as in $\mathbf{p}$. We use the notation $\hat{u}$ for unit vectors. For the differential volume element we use $d\mathbf{p}$. In spherical coordinates the differential volume element is given by $d\mathbf{p} = p^2 dp d\hat{p}$. Our notation of $d\hat{p}$ is the differential element for the solid angle and is usually denoted as $d\Omega$. In the case of spherical coordinates $d\hat{p} = \sin\theta d\theta d\phi$, where θ is the polar angle and ϕ is the azimuthal angle. Likewise the arguments of the spherical harmonics are indicated by $\hat{p}$. For example, the argument of $Y_l^m(\hat{p})$ would represent the angles θ and ϕ associated with the vector $\mathbf{p}$.

Chapter 1

INTRODUCTION

In this chapter we review the history of the atomic model, we provide a review of the fundamental forces of nature, and we discuss the Sucher equation and its application to the charmonium and bottomonium meson systems.

1.1 Historical Overview of Atomic Models

Perhaps the earliest model of the atom was proposed by the ancient greeks, Democritus and Leucippus, at roughly 450 B.C. [2, 3, 4]. Democritus proposed that atoms were the smallest unit of matter, but were indivisible. It was thought that an infinite number of atoms could exist and that each atom differed from others in its size and shape. The position of an atom relative to other atoms was also an important aspect of this early theory. Democritus also hypothesized that atoms were always in motion, an idea derived from philosophical views of the heavens. From this idea, Democritus theorized that matter was composed of various atoms in perpetual motion. As was the case with many Greek philosophers, Democritus and Leucippus were intellectually ahead of their time. It would not be for another 2000 years before scientists would develop new models of the atom.

John Dalton made the next step toward developing the modern view of the atom. In the early 1800's Dalton [5] proposed the idea that compounds, the building blocks of molecules, were composed of elements. He stated that elements were composed of atoms which could be distinguished by atomic weight. Each element was believed to be composed of identical atoms. Unfortunately for Dalton, very few elements were known during his time. However, by the mid 1800's, many elements had been discovered. Mendeleev was able to construct the periodic table by carefully organizing the chemical properties of the elements. But the idea of atoms as being indivisible particles would soon change.

By the late 1800's J.J. Thomson had measured the charge to mass ratio of the electron [6] and proprosed a plum pudding model of the atom. In the plum pudding model, negatively charged *corpuscles* (later known as electrons) are embedded in a uniform positively charged sphere. The negative charges of the corpuscles canceled those of the surrounding positive charge resulting in a neutral atom.

Some of the greatest advances in the nuclear model took place during the beginning of the twentieth century [6, 7, 8, 9, 10]. In the early 1900's Max Planck had proposed the idea that electromagnetic radiation existed in discrete energy packets called quanta. Planck introduced

the concept of a quanta, where the energy is given as $E = nh\nu$, where h is Planck's constant, ν is the frequency, and n is an integer indicating that the energy is discrete. The quantization of electromagnetic radiation was eventually used to explain the ultra-violet catastrophe problem that existed in previous theoretical predictions of radiation from perfect black-bodies. Other experiments, such as the photoelectric effect, provided additional support for the quantization idea.

As the ideas of quantum physics developed, other important discoveries were made. Although J.J. Thomson had measured the charge to mass ratio of the electron, the exact charge and mass were not yet known. Robert Millikan developed an oil drop experiment to determine the charge of the electron. That information combined with the charge to mass ratio could be used to predict the electron's mass. During the early 1900's Rutherford developed an experiment in which alpha particles were used to bombard the gold atom. One would expect that the electrons, being much less massive than the alpha particles, would interact only weakly. Most of the alpha particles streamed through the gold plate, but others were scattered obliquely. This suggested that the atom consisted of concentrated positive charges located in mostly empty space. This research eventually led to the discovery of the proton.

Bohr had begun to develop his model of the atom. The Bohr model of the atom consists of negatively charged electrons in orbit about a positively charged nucleus. Bohr used the idea that the electrons would move in circular orbits about the nucleus. In keeping with the new developments of quantization, Bohr proposed that excitations in the atom could be caused by the transition of the electrons from lower to higher energy levels. The energy levels were not continuous, but discrete. Only an exact amount of photon energy could be absorbed to make a transition from a lower energy state to a higher energy state. In addition, the electrons could make transitions from excited states to lower energy states by emitting a discrete amount of energy in the form of photons. The Bohr model is depicted in figure (1.1). The ground state energy is represented by $n = 1$ and the first two excited states are labeled as $n = 2$ and $n = 3$. We represent the energy of the orbit as E_n. In order for an electron to make a transition from the ground state to the first excited state, it must absorb a photon with energy $E = E_2 - E_1$, whereas a photon with energy $E = E_3 - E_1$ most be absorbed for the electron to make a transition from the ground state to the second excited state. Likewise, an electron making a transition from the second excited state to the ground state would emit a photon of energy $E = E_3 - E_1$. The Bohr model was used to successfully predict the hydrogen spectrum. Confirmation of the discrete energy levels in the Bohr model followed from the Frank-Hertz experiment.

Although the Bohr model was successful in many ways, it did not always agree with experiment. The Bohr model was not very successful in the prediction of the spectral lines for more complicated atoms. It couldn't be used to predict the relative intensities of spectral lines. In addition, it did not predict the odd splitting in the spectral lines that we now know results from relativistic effects. Wilson and Sommerfield made modifications to the Bohr model which

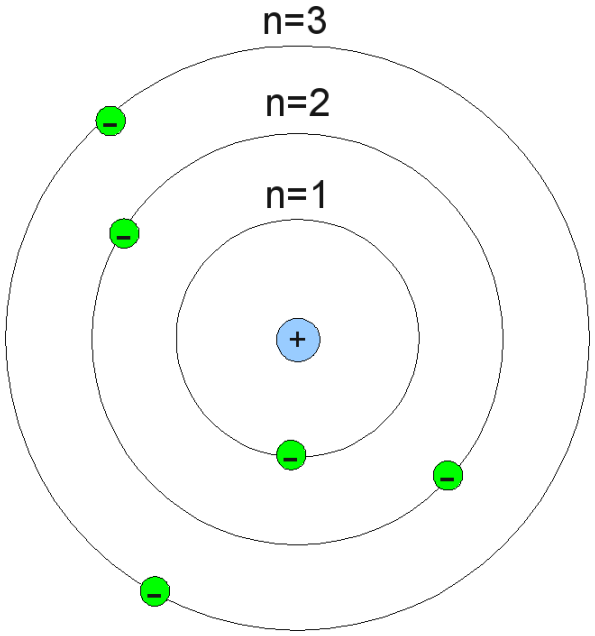

Figure 1.1: Bohr Model of the atom. Negatively charged electrons move in circular orbits about a positively charged nucleus. Electrons may make transitions by absorbing or emitting photons.

led to more accurate predictions of atomic spectra with limited success. These shortcomings implied that better treatment was needed.

Concurrent theoretical developments by Albert Einstein in the early 1900's led to the Special and General Theories of Relativity. The Special Theory of Relativity is summarized in two postulates [7]: (1) The laws of physics are the same in all inertial reference frames moving at relative constant velocities. (2) The speed of light in a vacuum is constant and it does not depend of the motion of the observer or the light source. These postulates led to results outside the purview of the human observational experience. Length contraction, time dilation, and relativistic variations in mass were byproducts of Einstein's Special Theory of Relativity. If we write the momentum in a 4-vector covariant form, then we can easily show that the energy/mass relation is given as $E^2 = m^2c^4 + p^2c^2$, where E is the energy, c is the speed of light, and p is the magnitude of the 3 momentum. The rest mass energy is given by $E = mc^2$. Michelson and Morley devised an experiment which measured the speed of light to be a constant, dispelling the belief that the speed of light was infinite and confirming Einstein's idea. The effects of special relativity have been experimentally verified [11, 12, 13].

Using the experimental evidence that light had characteristics of particles and waves, in 1924 de Broglie suggested that the electron may have similar properties. His work led to the belief that energy quantization could be explained from wave theory [5, 6, 7, 14, 15]. In 1925 Erwin Schrödinger published his work on the wave equation, which would later become known as the Schrödinger equation. In this model, the wave function is the probability amplitude of finding a particle at a specific position or momentum. This is different from the classical and semi-classical models developed by Bohr and others in that a particle's position is not completely

deterministic; one may only specify the probability of a particle's position. Werner Heisenberg also developed matrix mechanics which was later shown to be equivalent to Schrödinger's theory. The Heisenberg uncertainty principle forbids precise knowledge of both position and momentum simultaneously. The Schrödinger equation was used to predict the spectra of Hydrogen and also of more complicated atoms.

The Schrödinger equation is useful in prediction mass spectra, however fine structure and hyperfine splitting of atom spectra were still not well understood. The genesis of spin begin with the point-like classical ideal of particles. If one considers the proton and electron of the hydrogen atom and allows for the particles to rotate about their own axes as well as about their common center of mass, then the electron and proton can generate magnetic moments. The *spin* of the proton is proportional to its magnetic moment. Likewise the *spin* of the electron is proportional to the electron's magnetic moment. The interaction of the electron and proton spin would be known as spin-spin interaction. If one were viewing the electron from the perspective of the proton, then the spin of the proton would be proportional to the angular momentum vector of electron's orbit about the proton [8]. This would be known as spin orbit-interaction. These two phenomenological interaction terms can be used in conjunction with the Schrödinger equation to produce the proper hyperfine and fine structure spectral line splittings. The existence of spin, however, had not been predicted from theory. The prediction of the existence of spin would come when Einstein's Special Theory of Relativity was combined with the wave equation of Schrödinger into a covariant theory.

In view of Einstein's discovery, space and time were to be treated on equal footing–meaning that time was an extra dimension that should be treated in the same manner as the spatial coordinates. Klein and Gordon made one of the earliest attempts to treat space and time in a covariant manner. The Klein-Gordon equation used second order spatial and second order temporal derivatives in its formulation. The second order temporal derivatives were not in agreement with Schrödinger's theory, and the Klein-Gordon equation did not predict the existence of spin. In 1928 Paul Dirac published his theory which combined Einstein's Special Theory of Relativity with the quantum mechanical treatment of half integral spin particles. Dirac's equation explained the existence of spin in its formulation. There was some confusion in the interpretation of the Dirac's equation, because both negative and positive energy states were predicted. However the negative energy states were eventually interpreted as antiparticles. The existence of antiparticles was confirmed when Carl Anderson discovered the positron in 1932, the same year in which the neutron was discovered.

In the early 1930's the basic structure of the atom had been established. However, the physics that governs the interaction of nucleons had not been formulated. Japanese physicist Yukawa proposed that nucleons interact by exchanging mesons. Yukawa predicted that the mass of the meson should be roughly 300 times the electron's mass to account for the short range of interaction. (In contrast the electromagnetic interaction occurs by exchange of a massless

particle with infinite range, the photon.) A wealth of experimental evidence was exposed for the existence of mesons, as well as many other particles, in the remaining part of the twentieth century.

In 1961, Murray Gell-man and George Zweig proposed that hadrons were composed of elementary particles called quarks using their $SU(3)$ theory. Hadrons are classified as either baryons or mesons. Baryons are the bound states of three quarks and mesons are the bound state of a quark and antiquark. In 1968, scattering experiments at the Standford Linear Accelerator showed that the proton consisted of point like particles. This experiment was later interpreted as evidence for quarks, although no free quarks have ever been observed in nature. Since free quarks do not exist in nature, quarks are assigned a color. The color is used to ensure that constituent particles have a net color of white, also known as the color singlet or color neutral. Colors are quantum properties of the quarks and have nothing to do with our everyday notion of color. In addition, quarks have fractional charge. For example the up quark has charge $q = +2/3e$ and the down quark has charge $q = -1/3e$, where e is the charge of the electron. Thus two up quarks and one down quark can be used to account for the proton charge of $q = +1$. Gluons, the force carrying particles of the strong interaction, possess color charge. For this reason gluons interact with quarks and with other gluons (self interaction).

1.2 The Fundamental Forces

The four fundamental forces of nature are gravitation, weak, electromagnetic, and strong. Gravitational forces are believed to originate from the exchange of a vector boson known as the graviton. The weak force, which governs radiative decay, is mediated by the exchange of the massive W and Z bosons. The electromagnetic force is mediated by the exchange of photons, and the strong force is mediated by the exchange of gluons.

Quantum electrodynamics (QED) is the physical theory that describes the interaction of matter with light [16, 17]. In quantum field theory, quantization conditions are imposed on the system. In perturbation theory, one can derive diagrams called the Feynman diagrams. In this theory, the fundamental interaction is that of two fermions exchanging a photon while satisfying the conservation of momentum. All possible interactions between fermions and photons can be shown is this way. The Coulomb interaction is only an approximation derived from the Feynman diagrams of QED at low energy. The fine structure coupling constant $\alpha = 1/137$ makes QED a useful perturbation theory and is perhaps the most accurate theory in physics [18].

Quantum Chromodynamics (QCD) is the theory that describes the interaction of quarks and gluons. Since gluons possess color charge, they participate in self-interaction and in the interaction of quarks. In 1973, David Gross, David Politzer, and Frank Wilczek derived the property known as asymptotic freedom [18]. In QCD, quarks behave as essentially free particles and participle in one gluon exchange (OGE) at high energies. The one gluon exchange allows for

one to derive a Coulomb-like potential for short range interaction. However, at lower energies (larger seperation distances between quarks) the self interaction of the gluons combined with the quark-gluon interaction is such that the quarks remain confined. The nature of confinement is an open area of research.

1.3 The Sucher Equation

We have described a number of different atomic models including the Bohr model, the Dirac equation, and the Schrödinger equation. There have been other theories that can be used for the study of bound state spectra. In this dissertation, we study the charmonium and bottomonium mesons using the Sucher equation, which has never been used for meson mass spectra. The Sucher equation is relativistic and contains spin dependence in its formulation. We derive the Sucher equation from the sum of the Dirac Hamiltonians with a two-body interaction modified by positive energy projectors. Without the positive energy projectors, the two-body interaction gives rise to a condition known as Brown-Ravenhall disease [19]. Brown and Ravenhall showed that there is no lower bound on the energy and that the wave functions cannot be normalized when using a two-body interaction. To model to the two-body interaction, we use the Coulomb-like potential derived from asymptotic freedom, and we use a linear potential for confinement.

In the next chapter, we provide a derivation and a full angular momentum analysis of the Sucher equation. A full angular momentum analysis of the Sucher equation has never been studied. We begin by reviewing the Schrödinger equation in the position space, mixed space, and momentum space representations. The techniques we use to solve the Schrödinger equation will be usefull for our analysis of the Sucher equation.

Chapter 2

THEORY

In this section, we express the Schrödinger equation in three representations. Moreover, we derive the Sucher equation, and we perform a full angular momentum analysis showing that spin-spin, spin-orbit, and tensor interactions are inherent to the equation. The Sucher equation is a relativistic equation, and it will be solved in the momentum space representation. For this reason, the solutions to the Schrödinger equation and the methods used to solve it will provide insight into solving the Sucher equation.

2.1 The Schrödinger Equation

One way of predicting meson spectra is to use the Schrödinger equation. The Schrödinger equation is written

$$\hat{H}|\psi\rangle = E|\psi\rangle \tag{2.1}$$

where $\hat{H}$ is the Hamiltonian operator, E is the energy and $|\psi\rangle$ is the state vector. The Schrödinger equation can be written in three different representations: position space, mixed-space, and momentum space. The Hamiltonian is written as $\hat{H} = \hat{T} + \hat{V}$. The non-relativistic kinetic energy operator is $\hat{T} = \hat{p}^2/2\mu$ where μ is the reduced mass of the two body system and $\hat{p}$ is momentum operator. The relativistic kinetic energy operator is written $\hat{T}(p) = \sqrt{\hat{p}^2 + m_1^2} + \sqrt{\hat{p}^2 + m_2^2}$ where m_1 are m_2 are the masses of the particles, and we have used units in which $\hbar = c = 1$.

2.2 Schrödinger Equation in Position Space

To derive the position space representation of the Schrödinger equation, we write

$$\langle \mathbf{r}|\hat{T}|\psi\rangle + \langle \mathbf{r}|\hat{V}|\psi\rangle = E\langle \mathbf{r}|\psi\rangle. \tag{2.2}$$

If we use the non-relativistic kinetic energy operator, then the Schrödinger equation becomes

$$\langle \mathbf{r}|\frac{\hat{p}^2}{2\mu}|\psi\rangle + \langle \mathbf{r}|\hat{V}|\psi\rangle = E\langle \mathbf{r}|\psi\rangle. \tag{2.3}$$

Next we use completeness over the position basis vectors to write

$$\int \langle \mathbf{r}|\frac{\hat{p}^2}{2\mu}|\mathbf{r}'\rangle\langle \mathbf{r}'|\psi\rangle d\mathbf{r}' + \int \langle \mathbf{r}|\hat{V}|\mathbf{r}'\rangle\langle \mathbf{r}'|\psi\rangle d\mathbf{r}' = E\langle \mathbf{r}|\psi\rangle. \tag{2.4}$$

We use the following

$$\langle \mathbf{r}|\hat{p}|\mathbf{r}'\rangle = -i\hat{\boldsymbol{\nabla}}_r\delta(\mathbf{r}-\mathbf{r}'), \tag{2.5}$$

to write the Schrödinger equation as

$$\int \frac{-\nabla_r^2}{2\mu}\delta(\mathbf{r}-\mathbf{r}')\langle\mathbf{r}'|\psi\rangle d\mathbf{r}' + \int \langle\mathbf{r}|\hat{V}|\mathbf{r}'\rangle\langle\mathbf{r}'|\psi\rangle d\mathbf{r}' = E\langle\mathbf{r}|\psi\rangle. \tag{2.6}$$

Next we assume that the potential is local (i.e. a function of the magnitude of the relative distance between the particles), so $\langle\mathbf{r}|\hat{V}|\mathbf{r}'\rangle = V(r)\delta(\mathbf{r}-\mathbf{r}')$. Using the local potential and the definition of the position space wave function $\langle\mathbf{r}|\psi\rangle$, the above equation becomes

$$\int \frac{-\nabla_{r'}^2}{2\mu}\delta(\mathbf{r}-\mathbf{r}')\psi(\mathbf{r}')d\mathbf{r}' + \int V(r)\delta(\mathbf{r}-\mathbf{r}')\psi(\mathbf{r}')d\mathbf{r}' = E\psi(\mathbf{r}). \tag{2.7}$$

Finally we evaluate the delta functions and arrive at the position space Schrödinger equation

$$-\frac{\nabla_r^2}{2\mu}\phi(\mathbf{r}) + V(r)\phi(\mathbf{r}) = E\phi(\mathbf{r}) \tag{2.8}$$

We use separation of variables such that $\psi(\mathbf{r}) = R_l(r)Y_l^m(\hat{r})$ where $R_l(r)$ is a function of r and $Y_l^m(\hat{r})$ are the spherical harmonics. The angular momentum is a good quantum number and is given by l. The z projection of angular momentum is labeled m. If we define a reduced wave function as $u_l(r) = rR_l(r)$, we may write the radial part of the Schrödinger equation as

$$-\frac{1}{2\mu}\frac{d^2u_l(r)}{dr^2} + \frac{l(l+1)}{2\mu r^2}u_l(r) + V(r)u_l(r) = Eu_l(r). \tag{2.9}$$

Next we write the Schrödinger equation in the mixed space representation.

2.3 Schrödinger Equation in Mixed Space

In the mixed-space representation, the kinetic energy operator is treated in momentum space and the potential energy operator is in position space. To derive the mixed space representation we start the with the Hamiltonian and project from the left with a momentum space vector

$$\langle\mathbf{p}|\hat{T}(\hat{p})|\psi\rangle + \langle\mathbf{p}|\hat{V}|\psi\rangle = E\langle\mathbf{p}|\psi\rangle. \tag{2.10}$$

For the kinetic energy term, we insert completeness over momentum resulting in

$$\int \langle\mathbf{p}|\hat{T}(\hat{p})|\mathbf{p}'\rangle\langle\mathbf{p}'|\psi\rangle d\mathbf{p}' + \langle\mathbf{p}|\hat{V}|\psi\rangle = E\langle\mathbf{p}|\psi\rangle, \tag{2.11}$$

where upon acting with the kinetic energy operator we obtain

$$\int T(p')\psi(\mathbf{p}')\delta(\mathbf{p}-\mathbf{p}')d\mathbf{p}' + \langle\mathbf{p}|\hat{V}|\psi\rangle = E\psi(\mathbf{p}). \tag{2.12}$$

Next we evaluate the delta function

$$T(p)\psi(\mathbf{p}) + \langle\mathbf{p}|\hat{V}|\psi\rangle = E\psi(\mathbf{p}).. \tag{2.13}$$

We then insert completeness over position

$$T(p)\psi(\mathbf{p}) + \int \langle \mathbf{p}|\mathbf{r}\rangle \langle \mathbf{r}|\hat{V}|\mathbf{r}'\rangle \langle \mathbf{r}'|\psi\rangle d\mathbf{r}d\mathbf{r}' = E\psi(\mathbf{p}). \tag{2.14}$$

We use the plane wave representation, $\langle \mathbf{p}|\mathbf{r}\rangle = e^{-i\mathbf{p}\cdot\mathbf{r}}/(2\pi)^{3/2}$.

$$T(p)\psi(\mathbf{p}) + \int \frac{e^{-i\mathbf{p}\cdot\mathbf{r}}}{(2\pi)^{3/2}} \langle \mathbf{r}|\hat{V}|\mathbf{r}'\rangle \psi(\mathbf{r}')d\mathbf{r}d\mathbf{r}' = E\psi(\mathbf{p}). \tag{2.15}$$

Again, we assume that the potential is local

$$T(p)\psi(\mathbf{p}) + \int \frac{e^{-i\mathbf{p}\cdot\mathbf{r}}}{(2\pi)^{3/2}} V(r)\psi(\mathbf{r})d\mathbf{r} = E\psi(\mathbf{p}). \tag{2.16}$$

Decomposing the wave functions and using the plane wave expansion [20],

$$e^{-i\mathbf{p}\cdot\mathbf{r}} = 4\pi \sum_{l',m'} (-i)^{l'} j_{l'}(pr) Y_{l'}^{m'}(\hat{p}) Y_{l'}^{*m'}(\hat{r}), \tag{2.17}$$

we find the above equation becomes

$$\begin{aligned} &T(p)\psi_l(p)Y_l^m(\hat{p}) + \\ &\quad \sqrt{\frac{2}{\pi}} \sum_{l',m'} \int (-i)^{l'} j_{l'}(pr) Y_{l'}^{*m'}(\hat{r}) Y_{l'}^{m'}(\hat{p}) V(r) \psi_l(r) Y_l^m(\hat{r}) r^2 dr d\hat{r} \\ &\quad = E\psi_l(p)Y_l^m(\hat{p}). \end{aligned} \tag{2.18}$$

After integrating over the angles we find

$$T(p)\psi_l(p) + \sqrt{\frac{2}{\pi}} \int_0^\infty (-i)^l j_l(pr)\psi_l(r)V(r)r^2 dr = E\psi_l(p). \tag{2.19}$$

At this point one could absorb the phase factor $-i^l$ into the wave function since this would not change the probability given by $|\psi|^2$. We will absorb the phase factor into the coefficients when we apply the variational principle to this equation. For this discussion, see section 2.5.2. Next, we will write the Schrödinger equation in the momentum space representation.

2.4 Schrödinger Equation in Momentum Space

In addition to solving the Schrödinger equation in the position space and mixed space representations, one may also solve the Schrödinger equation in the momentum space representation. To derive the p-space equation we start by projecting with the momentum space vector as we did when deriving the mixed space Schrödinger equation. Therefore we will obtain equation (2.13)

$$T(\mathbf{p})\psi(\mathbf{p}) + \langle \mathbf{p}|\hat{V}|\psi\rangle = E\psi(\mathbf{p}).$$

We use completeness in momentum space to write

$$T(p)\psi(\mathbf{p}) + \int \langle \mathbf{p}|\hat{V}|\mathbf{p}'\rangle \psi(\mathbf{p}')d\mathbf{p}' = E\psi(\mathbf{p}). \tag{2.20}$$

As before, we decompose the wave function as $\psi(\mathbf{p}) = \psi_l(p)Y_l^m(\hat{p})$ where l is a good quantum number, and we expand the potential in terms of spherical harmonics

$$V(\mathbf{p},\mathbf{p}') = V(\mathbf{q}) = \sum_{l'm'} V_{l'}(p,p')Y_{l'}^{m'}(\hat{p})Y_{l'}^{*m'}(\hat{p}'), \tag{2.21}$$

such that

$$\begin{aligned} T(p)\psi_l(p)Y_l^m(\hat{p}) & \\ &+ \sum_{l'm'} \int V_{l'}(p,p')Y_{l'}^{m'}(\hat{p})Y_{l'}^{*m'}(\hat{p}')\psi_l(p')Y_l^m(\hat{p}')p'^2 dp' d\hat{p}' \\ &= E\psi_l(p)Y_l^m(\hat{p}). \end{aligned} \tag{2.22}$$

Finally, we integrate over the angles, and the result is the lth partial wave momentum space Schrödinger equation

$$T(p)\psi_l(p) + \int_0^\infty V_l(p,p')\phi(p')p'^2 dp' = E\psi_l(p). \tag{2.23}$$

The Fourier transform of the r-space potential $V(\mathbf{q})$ is related to $V_l(p,p')$ by

$$V_l(p,p') = 2\pi \int_{-1}^{1} V(\mathbf{q})P_l(x)dx, \tag{2.24}$$

where $\mathbf{q} = \mathbf{p} - \mathbf{p}'$ is the momentum transfer, $x = cos(\theta_{pp'})$ and $\theta_{pp'}$ is the angle between $\mathbf{p}$ and $\mathbf{p}'$. Now that we have written the Schrödinger equation in the three representations, we will show how the variational principle can be used to solve for the energies and wave functions.

2.5 Applying the Variational Principle

We will expand the wave functions in each of the three representations as a complete set of basis functions. Then we will write the Schrödinger equation as matrix equation. The variational principle is used to find the eigenvalues and eigenvectors. We associate the eigenvalues with the energy and the eigenvectors with the coefficients of the wave function expansion. We use the coefficients to reconstruct the wave functions. A full discussion of the variational principle appears in Appendix A.

2.5.1 Schrödinger Equation in Position Space

To apply the variational principle, we will first expand $u_l(r)$ from equation (2.9) in terms of a complete orthonormal set of basis functions.

$$u_l(r) = \sum_j g_j^l(r)c_j, \tag{2.25}$$

where $g_j^l(r)$ are chosen to satisfy the boundary conditions, c_j are the coefficients, and the orthogonality condition satisfies

$$\int_0^\infty g_i^l(r)g_j^l(r)dr = \delta_{ij}. \tag{2.26}$$

If we substitute this into the r-space Schrödinger equation and project from the left with $g_i^l(r)$ and integrate over dr, then

$$\sum_j \left[\int_0^\infty g_i^l(r) \frac{-1}{2\mu} \frac{d^2}{dr^2} g_j^l(r) + \int_0^\infty g_i^l(r) g_j^l(r) r^2 dr \right] c_j = E c_i, \tag{2.27}$$

where we have used the orthogonality condition. If we define

$$H_{ij} = \left[\int_0^\infty g_i^l(r) \frac{-1}{2\mu} \frac{d^2}{dr^2} g_j^l(r) + \int_0^\infty g_i^l(r) g_j^l(r) r^2 dr \right], \tag{2.28}$$

then we can write $\sum_j H_{ij} = E c_i$ which we can represent as a matrix equation $\tilde{H}\mathbf{c} = E\mathbf{c}$.

If we had chosen to use the relativistic kinetic energy operator in which $\hat{T}(p) = \sqrt{\hat{p}^2 + m_1^2} + \sqrt{\hat{p}^2 + m_2^2}$ then we would have had a spatial derivative operator beneath the radicals when $\mathbf{p} \to i\nabla$. In this case, to the solve the position space Schrödinger equation one needs to expand the radical in a Taylor series. Such an approximation is suitable for heavy mass systems, but it would not be productive for light particle systems. One may choose to solve the Schrödinger equation in a different representation in which the kinetic energy operator is acting in momentum space. In momentum space the kinetic energy operator is a number, thus it would pose no problem beneath the radical.

2.5.2 Schrödinger Equation in Mixed Space

Next we expand the wave functions from equation (2.19) in a complete orthonormal set of basis functions

$$\psi_l(p) = \sum_j \tilde{g}_j^l(p) \tilde{c}_j \qquad \psi_l(r) = \sum_j g_j^l(r) c_j, \tag{2.29}$$

where $g_j^l(r)$ and $\tilde{g}_j^l(p)$ are the functions that satisfy the boundary conditions and c_j and $\tilde{c}_j$ are the coefficients. In order to represent the Schrödinger equation in the mixed space representation, $\tilde{g}_j^l(p)$ and $g_j^l(r)$ must be a Fourier-Bessel transform pair,

$$\tilde{g}_j^l(p) = \sqrt{\frac{2}{\pi}} \int_0^\infty j_l(pr) g_j^l(r) r^2 dr \tag{2.30}$$

and

$$g_j^l(r) = \sqrt{\frac{2}{\pi}} \int_0^\infty j_l(pr) \tilde{g}_j^l(p) p^2 dp. \tag{2.31}$$

which satisfy the following orthonormality conditions

$$\int_0^\infty \tilde{g}_i^l(p) \tilde{g}_j^l(p) p^2 dp = \delta_{ij} \tag{2.32}$$

and

$$\int_0^\infty g_i^l(p) g_j^l(p) p^2 dp = \delta_{ij}. \tag{2.33}$$

Expanding the wave functions as in (2.29), we may write equation (2.19) as

$$\sum_j T(p)\tilde{g}_j^l(p)\tilde{c}_j + \sum_j \int_0^\infty (-i)^l j_l(pr) g_j^l(r) r^2 V(r) dr c_j = E \sum_j \tilde{g}_j^l(p)\tilde{c}_j. \tag{2.34}$$

We define $c_j = (i)^l \tilde{c}_j$, and we project with $\tilde{g}_i^l(p)p^2$ and integrate over dp

$$\begin{aligned} \sum_j \Bigg[\int_0^\infty p^2 T(p)\tilde{g}_i^l(p)\tilde{g}_j^l(p)dp & \\ + \int j_l(pr)\tilde{g}_i^l(p) g_j^l(r) p^2 r^2 V(r) dr dp \Bigg] c_j & \\ = E \sum_j \int_0^\infty \tilde{g}_i^l(p)\tilde{g}_j^l(p) p^2 dp\, c_j. & \end{aligned} \tag{2.35}$$

Next we insert equation (2.30)

$$\begin{aligned} \sum_j \Bigg[\int p^2 T(p)\tilde{g}_i^l(p)\tilde{g}_j^l(p)dp & \\ + \int_0^\infty j_l(pr) j_l(pr') g_i^l(r) g_j^l(r) V(r) r^2 r'^2 p^2 dr dr' dp \Bigg] c_j & \\ = E \sum_j \int_0^\infty \tilde{g}_i^l(p)\tilde{g}_j^l(p) p^2 dp\, c_j & \end{aligned} \tag{2.36}$$

Finally we integrate over dp and by using the following integral [20]

$$\int_0^\infty r^2 j_l(pr) j_l(pr') p^2 dp = \frac{\pi}{2r^2}\delta(r-r') \tag{2.37}$$

and the orthogonality conditions. We arrive with the mixed space Schrödinger equation

$$\sum_j \Bigg[\int p^2 T(p)\tilde{g}_i^l(p)\tilde{g}_j^l(p)dp \tag{2.38}$$

$$+ \int_0^\infty g_i^l(r) g_j^l(r) V(r) r^2 dr \Bigg] c_j = E c_i. \tag{2.39}$$

As in the position space representation, we may write

$$H_{ij} = \int_0^\infty p^2 T(p)\tilde{g}_i^l(p)\tilde{g}_j^l(p)dp + \int_0^\infty g_i^l(r) g_j^l(r) V(r) r^2 dr, \tag{2.40}$$

such that

$$\sum_j H_{ij} c_j = E c_i. \tag{2.41}$$

We can represent this as a matrix equation $\tilde{H}\mathbf{c} = E\mathbf{c}$.

2.5.3 Schrödinger Equation in Momentum Space

Again, for the momentum space representation, we will expand the wave function in a complete set of orthonormal basis functions,

$$\psi_l(p) = \sum_j g_j^l(p) c_j \tag{2.42}$$

where $g_j^l(p)$ where $g_j^l(p)$ is chosen to satisfy the boundary conditions and c_j are coefficients. The functions satisfy the normalization condition

$$\int g_i^l(p) g_j^l(p) p^2 dp = \delta_{ij}. \tag{2.43}$$

We may then write the momentum space Schrödinger equation as

$$\sum_j H_{ij} c_j = E c_i \tag{2.44}$$

where

$$H_{ij} = \int_0^\infty T(p) g_i^l(p) g_j^l(p) p^2 dp + \int g_i^l(p) g_j^l(p') V_l(p,p') p^2 p'^2 dp' dp. \tag{2.45}$$

Again, we may represent this a matrix equation $\tilde{H}\mathbf{c} = E\mathbf{c}$.

For each the three different representations, we were able to write the Schrödinger equation in terms of a matrix equation,

$$\tilde{H}\mathbf{c} = E\mathbf{c}. \tag{2.46}$$

We solve for the matrix equation for the eigenvalues and eigenvectors. We then use the eigenvalues as the energy, and we use to the eigenvectors c_j to reconstruct the wave function by using equation (2.42)

We have written the Schrödinger equation in the position space, mixed space, and momentum space representations. In the next section, we will derive a relativistic equation in momentum space known as the Sucher equation. Similar methods are used for the partial wave decomposition.

2.6 Deriving the Sucher Equation

In this section, we will derive the Sucher equation [21]. We begin by considering the sum of the free Dirac Hamiltonians for a two-body system,

$$H_{\text{Free}} = H_D(1) + H_D(2) = \sum_{i=1}^{2} (\mathbf{p} \cdot \boldsymbol{\alpha}_i + \boldsymbol{\beta} m_i), \tag{2.47}$$

where the subscript i represents the particle number, $\mathbf{p}$ is the momentum, $\boldsymbol{\alpha}$ is given by

$$\boldsymbol{\alpha}_i = \begin{pmatrix} \mathbf{0} & \boldsymbol{\sigma}_i \\ \boldsymbol{\sigma}_i & \mathbf{0} \end{pmatrix} \tag{2.48}$$

where $\boldsymbol{\sigma} = \sigma^x\hat{x} + \sigma^y\hat{y} + \sigma^z\hat{z}$ where σ^x, σ^y, and σ^z are the Pauli spin matrices, the $\mathbf{0}$'s are 2×2 zero matrices, and $\boldsymbol{\beta}$ is given by

$$\boldsymbol{\beta} = \begin{pmatrix} \mathbf{1} & \mathbf{0} \\ \mathbf{0} & -\mathbf{1} \end{pmatrix} \tag{2.49}$$

where $\mathbf{1}$ represents the 2×2 diagonal identity matrix. Note that in our convention, superscripts indicate components of the Pauli spin matrices σ^x, σ^y. and σ^z and subscripts of $i = 1$ or $i = 2$ indicates the particle label. Since we will be using the Sucher equation for quarkonium bound states, we need to add the two body interaction. Thus the Hamiltonian becomes

$$H = H_{\text{Free}} + V_{12} \tag{2.50}$$

where V_{12} is the two body interaction. Brown and Ravenhall [19] showed that the two body interaction V_{12} gives rise to a condition in which no lower bound of the energy states can be achieved. This also leads to wave functions which cannot be normalized. We may modify the potential such that the negative energy states are omitted. This is achieved by using positive energy projectors as defined by

$$\Lambda_+(i) = \frac{E_i + (\mathbf{p}\cdot\boldsymbol{\alpha}_i + \boldsymbol{\beta} m_i)}{2E_i}, \tag{2.51}$$

where E_i is the relativistic energy given by $E_i = \sqrt{p^2 + m_i^2}$. Using the positive energy projectors, the modified two-body potential (no-pair) potential is given by [21]

$$V_{++} = \Lambda_+(1)\Lambda_+(2)V_{12}\Lambda_+(1)\Lambda_+(2). \tag{2.52}$$

The positive and negative energy projectors are discussed in Appendix B. The Hamiltonian for the Sucher Equation with a modified two-body potential is given by $H_{\text{S}} = H_D(1) + H_D(2) + V_{++}$. Next we operate with Hamiltonian onto the state vector ψ giving $H_S|\psi\rangle = E|\psi\rangle$. Sucher defines the state vector as $|\psi\rangle = \mathbf{S}_1\mathbf{S}_2|\phi\rangle$, where

$$\mathbf{S}_i = (\mathbf{1} + \boldsymbol{\xi}_i)\boldsymbol{\beta}^+ A_i \qquad \xi = \frac{\boldsymbol{\alpha}_i\cdot\mathbf{p}}{E_i + m_i} \tag{2.53}$$

and

$$A_i = \sqrt{\frac{E_i + m_i}{2E_i}} \qquad \boldsymbol{\beta}^+ = \frac{\mathbf{1} + \boldsymbol{\beta}}{2}. \tag{2.54}$$

Now the Sucher Hamiltonian operating on the state $|\psi\rangle$ becomes

$$[H_D(1) + H_D(2) + \Lambda_+(1)\Lambda_+(2)V_{12}\Lambda_+(1)\Lambda_+(2)]\mathbf{S}_1\mathbf{S}_2|\phi\rangle = E\mathbf{S}_1\mathbf{S}_2|\phi\rangle. \tag{2.55}$$

If we express $\mathbf{S}_i$ and $\boldsymbol{\Lambda}_+(i)$ in matrix form we can show that

$$\boldsymbol{\Lambda}_+(i)\mathbf{S}_i = A_i \begin{pmatrix} \mathbf{1} & \mathbf{0} \\ \frac{\boldsymbol{\sigma}_i\cdot\mathbf{p}}{E_i+m_i} & \mathbf{0} \end{pmatrix} = \mathbf{S}_i. \tag{2.56}$$

Using $\mathbf{\Lambda}_+(i)\mathbf{S}_i = \mathbf{S}_i$ and projecting through by $(\mathbf{S}_1\mathbf{S}_2)^\dagger = \mathbf{S}_2^\dagger\mathbf{S}_1^\dagger$ gives us

$$\mathbf{S}_2^\dagger\mathbf{S}_1^\dagger[H_D(1)+H_D(2)+\Lambda_+(1)\Lambda_+(2)V_{12}]\mathbf{S}_1\mathbf{S}_2|\phi\rangle = E\mathbf{S}_2^\dagger\mathbf{S}_1^\dagger\mathbf{S}_1\mathbf{S}_2|\phi\rangle \tag{2.57}$$

Next, using the definitions of $\mathbf{S}_i$, we find

$$\mathbf{S}_i^\dagger\mathbf{S}_i = \frac{E_i+m_i}{2E_i}\begin{pmatrix}\frac{2E_i(E_i+m_i)}{(E_i+m_i)^2} & \mathbf{0}\\ \mathbf{0} & \mathbf{0}\end{pmatrix} = \begin{pmatrix}\mathbf{1} & \mathbf{0}\\ \mathbf{0} & \mathbf{0}\end{pmatrix} \tag{2.58}$$

We also find that

$$\mathbf{S}_i^\dagger\mathbf{\Lambda}_+ = A_i\begin{pmatrix}\mathbf{1} & \frac{\boldsymbol{\sigma}_i\cdot\mathbf{p}}{E_i+m_i}\\ \mathbf{0} & \mathbf{0}\end{pmatrix} = \mathbf{S}_i^\dagger. \tag{2.59}$$

Using the above results and the results of operating with the free Dirac Hamiltonian $H_D(i)|\phi\rangle = E_i|\phi\rangle$, where $E_i = \sqrt{p^2+m_i^2}$, equation (2.57) becomes

$$(E_1+E_2)|\phi\rangle + \mathbf{S}_2^\dagger\mathbf{S}_1^\dagger V_{12}\mathbf{S}_1\mathbf{S}_2|\phi\rangle = E\mathbf{S}_2^\dagger\mathbf{S}_1^\dagger\mathbf{S}_1\mathbf{S}_2|\phi\rangle. \tag{2.60}$$

Next we project with $\langle\mathbf{p}_1\mathbf{p}_2|$ on the above equation. (The notation indicates the tensor product of states: $|\mathbf{p}_1\mathbf{p}_1\rangle = |\mathbf{p}_1\rangle\otimes|\mathbf{p}_2\rangle$.)

$$\langle\mathbf{p}_1\mathbf{p}_2|(E_1+E_2)|\phi\rangle + \mathbf{S}_2^\dagger\mathbf{S}_1^\dagger V_{12}\mathbf{S}_1\mathbf{S}_2|\phi\rangle = E\langle\mathbf{p}_1\mathbf{p}_2|\phi\rangle, \tag{2.61}$$

where we have used equation (2.58) on the right-hand-side of the above equation. The wave function is then a function of the $\mathbf{p}_1$ and $\mathbf{p}_2$, since $\phi(\mathbf{p}_1,\mathbf{p}_2) = \langle\mathbf{p}_1\mathbf{p}_2|\phi\rangle$. Utilizing completeness over momentum, we find

$$\begin{aligned}(E_1+E_2)\phi(\mathbf{p}_1,\mathbf{p}_2) + \int\langle\mathbf{p}_1\mathbf{p}_2|\mathbf{S}_1^\dagger\mathbf{S}_2^\dagger|\mathbf{p_1''}\mathbf{p_2''}\rangle\langle\mathbf{p_1''}\mathbf{p_2''}|V_{12}|\mathbf{p_1'''}\mathbf{p_2'''}\rangle \\ \times\langle\mathbf{p_1'''}\mathbf{p_2'''}|\mathbf{S}_1\mathbf{S}_2|\mathbf{p_1'}\mathbf{p_2'}\rangle\phi(\mathbf{p_1'},\mathbf{p_2'})d\mathbf{p_1'}d\mathbf{p_2'}d\mathbf{p_1''}d\mathbf{p_2''}d\mathbf{p_1'''}d\mathbf{p_2'''} = E\phi(\mathbf{p_1},\mathbf{p_2}).\end{aligned} \tag{2.62}$$

After operating with $\mathbf{S}_i$, we evaluate the delta functions. For example, the first bracket results in $\mathbf{S}_i(\mathbf{p})$ multiplied by delta functions:

$$\langle\mathbf{p}_1\mathbf{p}_2|\mathbf{S}_1^\dagger\mathbf{S}_2^\dagger|\mathbf{p_1''}\mathbf{p_2''}\rangle = \mathbf{S}_1^\dagger(\mathbf{p_1''})\mathbf{S}_2^\dagger(\mathbf{p_2''})\delta(\mathbf{p_1''}-\mathbf{p_1})\delta(\mathbf{p_2''}-\mathbf{p_2}). \tag{2.63}$$

Using this we find that equation (2.63) becomes

$$\begin{aligned}(E_1+E_2)\phi(\mathbf{p_1},\mathbf{p_2}) + \int\mathbf{S}_1^\dagger(\mathbf{p_1})\mathbf{S}_1^\dagger(\mathbf{p_2})\langle\mathbf{p_1}\mathbf{p_2}|V_{12}|\mathbf{p_1'}\mathbf{p_2'}\rangle \\ \times\mathbf{S}_1^\dagger(\mathbf{p_1'})\mathbf{S}_1^\dagger(\mathbf{p_2'})\phi(\mathbf{p_1'},\mathbf{p_2'})d\mathbf{p_1'}d\mathbf{p_2'} = E\phi(\mathbf{p_1},\mathbf{p_2}).\end{aligned} \tag{2.64}$$

Next we make a transformation to the the center of momentum frame in which the relative momentum is written $\mathbf{p}$ and the total linear momentum is written $\mathbf{P}$. The transformation is obtained by using the Jacobian of the transformation $d\mathbf{p_1}d\mathbf{p_2} = J(\mathbf{p}_1\mathbf{p}_2,\mathbf{p},\mathbf{P})\; d\mathbf{p}d\mathbf{P}$, where the Jacobian in this case is $J(\mathbf{p}_1\mathbf{p}_2,\mathbf{p},\mathbf{P}) = 1$. In the center of momentum frame the total linear

momentum $\mathbf{P} = 0$, thus it is customary to write only the relative momentum. The Sucher equation in the center of momentum frame is given by

$$(E_1 + E_2)\phi(\mathbf{p}) + \int \mathbf{S}_1^\dagger(\mathbf{p})\mathbf{S}_2^\dagger(\mathbf{p})V_{12}(\mathbf{p},\mathbf{p}')\mathbf{S}_1(\mathbf{p}')\mathbf{S}_2(\mathbf{p}')\phi(\mathbf{p}')d\mathbf{p}' = E\phi(\mathbf{p}). \tag{2.65}$$

Next we compute the product of $\mathbf{S}_i^\dagger(\mathbf{p})\mathbf{S}_i(\mathbf{p}')$

$$\mathbf{S}_i^\dagger(\mathbf{p})\mathbf{S}_i(\mathbf{p}') = A_i^\dagger(\mathbf{p})A_i(\mathbf{p}')\begin{pmatrix} 1 + \frac{\boldsymbol{\sigma}_i\cdot\mathbf{p}}{E_i(\mathbf{p})+m_i}\frac{\boldsymbol{\sigma}_i\cdot\mathbf{p}'}{E_i(\mathbf{p}')+m_i} & \mathbf{0} \\ \mathbf{0} & \mathbf{0} \end{pmatrix} \tag{2.66}$$

Using the expression and for $\mathbf{S}_i^\dagger(\mathbf{p})\mathbf{S}_i(\mathbf{p}')$ and using $A_i^\dagger = A_i$, we find the Sucher equation in the center of momentum frame is given by [21]

$$\left(\sqrt{p^2+m_1^2} + \sqrt{p^2+m_2^2}\right)\phi(\mathbf{p}) + \int V^{\text{eff}}(\mathbf{p},\mathbf{p}')\phi(\mathbf{p}')d\mathbf{p}' = E\phi(\mathbf{p}), \tag{2.67}$$

where

$$\begin{aligned} V^{\text{eff}}(\mathbf{p},\mathbf{p}') = A_1(\mathbf{p})A_2(\mathbf{p})\Big[&V(\mathbf{q}) + \xi_1 V(\mathbf{q})\xi_1' + \xi_2 V(\mathbf{q})\xi_2' \\ &+\xi_1\xi_2 V(\mathbf{q})\xi_1'\xi_2'\Big]A_1(\mathbf{p}')A_2(\mathbf{p}') \end{aligned} \tag{2.68}$$

where A_i and ξ_i are given by equations (2.53) and (2.54), $\xi_i = \xi_i(\mathbf{p})$ and $\xi_i' = \xi_i'(\mathbf{p}')$, $\mathbf{q} = \mathbf{p} - \mathbf{p}'$ is the momentum transfer, and $V(\mathbf{q})$ is the Fourier transform of the r-space potential.

2.6.1 Angular Momentum Analysis

The Sucher equation is a three-dimensional integral equation in momentum space. In order to solve the Sucher equation, we will reduce the three-dimensional integral equation to a one-dimensional integral equation. First, we establish some new notation: The Sucher equation has the form

$$M(p)\phi(\mathbf{p}) = \int \hat{V}^{\text{eff}}(\mathbf{p},\mathbf{p}')\phi(\mathbf{p}')d\mathbf{p}', \tag{2.69}$$

where we define $M(p) = E - T(p)$ with E being the energy and T being the relativistic kinetic energy $T = \sqrt{p^2+m_1^2} + \sqrt{p^2+m_2^2}$. The effective potential for the Sucher equation is given by

$$\begin{aligned} V^{\text{eff}}(\mathbf{p},\mathbf{p}') &= A_1(\mathbf{p})A_2(\mathbf{p})[V^1 + (\boldsymbol{\sigma}_1\cdot\mathbf{p})V^2(\boldsymbol{\sigma}_1\cdot\mathbf{p}') \\ &+ (\boldsymbol{\sigma}_2\cdot\mathbf{p})V^3(\boldsymbol{\sigma}_2\cdot\mathbf{p}') \\ &+ (\boldsymbol{\sigma}_1\cdot\mathbf{p})(\boldsymbol{\sigma}_2\cdot\mathbf{p})V^4(\boldsymbol{\sigma}_1\cdot\mathbf{p}')(\boldsymbol{\sigma}_2\cdot\mathbf{p}')]A_1(\mathbf{p}')A_2(\mathbf{p}'), \end{aligned} \tag{2.70}$$

where

$$\begin{aligned} V^1 &= V(\mathbf{q}) \\ V^2 &= \frac{V(\mathbf{q})}{(E_1(\mathbf{p})+m_1)(E_1(\mathbf{p}')+m_1)} \\ V^3 &= \frac{V(\mathbf{q})}{(E_2(\mathbf{p})+m_2)(E_2(\mathbf{p}')+m_2)} \\ V^4 &= \frac{V(\mathbf{q})}{(E_1(\mathbf{p})+m_1)(E_2(\mathbf{p})+m_2)E_1(\mathbf{p}')+m_1)(E_2(\mathbf{p}')+m_2)}. \end{aligned} \tag{2.71}$$

The first step in finding the lth partial wave of the Sucher equation is to expand the wave function in terms of vector spherical harmonics. Since we are no longer assuming L is a good quantum number,

$$\phi(\mathbf{p}) = \sum_{L'S'M'J'} \phi_{L'}(p) \mathcal{Y}^{J'M'}_{L'S'}(\hat{p}), \tag{2.72}$$

where $\phi_L(p)$ is simplify a function of the magnitude of the momentum and $\mathcal{Y}^{JM}_{LS}(\hat{p})$ are the vector spherical harmonics. The vector spherical harmonics $\mathcal{Y}(\hat{p})$ may be written as a linear combination of the usual spherical harmonics $Y(\hat{p})$ and the spinors χ:

$$\mathcal{Y}^{JM}_{LS}(\hat{p}) = \sum_{m_L+m_S=M} \langle LSJM|lm_l Sm_S\rangle Y^{m_L}_L(\hat{p})\chi^{m_S}_S \tag{2.73}$$

where $J = L+S$ is the total angular momentum, L is the orbital angular momentum, S is the spin, M is the projection of the total angular momentum onto the z-axis, and bracket notation indicates a Clebsch-Gordan coefficient. The reason for expanding the wave function in this way is because the effective potential may couple angular momentum. The effect of the spin terms in the effective potential will manifest in its action on the vector spherical harmonics. In addition, the spin dependent terms may operate on the Fourier transform of the r-space potential $V(\mathbf{q})$. Therefore, we expand $V(\mathbf{q})$ in terms of a complete set of vector spherical harmonics.

$$V(\mathbf{q}) = \sum_{L_1 m_{L_1}} V_{L_1}(p,p') \mathcal{Y}^{J_1M_1}_{L_1S_1}(\hat{p}) \mathcal{Y}^{*J_1M_1}_{L_1S_1}(\hat{p}'). \tag{2.74}$$

Next, using equations (2.72) and (2.74), projecting from the left with $\mathcal{Y}^{*JM}_{LS}(\hat{p})d\hat{p}$ onto equation (2.69), and integrating over the $d\hat{p}$, we obtain

$$\begin{aligned} M(p)\phi_L(p) = \sum_{L'S'J'M'} \sum_{L_1S_1J_1M_1} \int & \mathcal{Y}^{*JM}_{LS}(\hat{p}) V^{\text{eff}}_{L_1}(p,p') \mathcal{Y}^{J_1M_1}_{L_1S_1}(\hat{p}) \mathcal{Y}^{*J_1M_1}_{L_1S_1}(\hat{p}') \\ & \times \phi_{L'}(p') \mathcal{Y}^{J'M'}_{L'S'}(\hat{p}') p'^2 dp' d\hat{p}' d\hat{p}, \end{aligned} \tag{2.75}$$

where $V^{\text{eff}}_{L_1}$ is given by

$$\begin{aligned} V^{\text{eff}}_{L_1}(\mathbf{p},\mathbf{p}') &= A_1(\mathbf{p})A_2(\mathbf{p})[V^1_{L_1} + (\boldsymbol{\sigma}_1\cdot\mathbf{p})V^2_{L_1}(\boldsymbol{\sigma}_1\cdot\mathbf{p}') \\ &+ (\boldsymbol{\sigma}_2\cdot\mathbf{p})V^3_{L_1}(\boldsymbol{\sigma}_2\cdot\mathbf{p}') \\ &+ (\boldsymbol{\sigma}_1\cdot\mathbf{p})(\boldsymbol{\sigma}_2\cdot\mathbf{p})V^4_{L_1}(\boldsymbol{\sigma}_1\cdot\mathbf{p}')(\boldsymbol{\sigma}_2\cdot\mathbf{p}')]A_1(\mathbf{p}')A_2(\mathbf{p}'). \end{aligned} \tag{2.76}$$

In the next sections, we will independently examine the V^1, V^2, V^3, and V^4 terms of the effective potential in equation (2.76), and we will write a general expression for the matrix elements of equation (2.75).

2.6.2 Effective Potential Term V^1

In this section we will compute the matrix element on the right hand side of equation (2.75) using the first term in the effective potential V^1 from equation (2.76). Using this, the right hand side of equation (2.75) is given by

$$\sum_{L_1S_1J_1M_1}\sum_{L'S'J'M'}\int A_1(\mathbf{p})A_2(\mathbf{p})\mathcal{Y}^{*JM}_{LS}(\hat{p})V^1_{L_1}(p,p')\mathcal{Y}^{J_1M_1}_{L_1S_1}(\hat{p})\mathcal{Y}^{*J_1M_1}_{L_1S_1}(\hat{p}') \tag{2.77}$$
$$\times\phi_{L'}(p')\mathcal{Y}^{J'M'}_{L'S'}(\hat{p}')A_1(\mathbf{p}')A_2(\mathbf{p}')p'^2dp'd\hat{p}'d\hat{p}.$$

Next, we will now carry out the integration over the angular variables $d\hat{p}$ and $d\hat{p}'$. We can represent the angular integration in terms of bracket notation

$$\int \mathcal{Y}^{*JM}_{LS}(\hat{p})\mathcal{Y}^{J_1M_1}_{L_1S_1}(\hat{p})d\hat{p} \rightarrow \langle LSJM|L_1S_1J_1M_1\rangle \tag{2.78}$$

and

$$\int \mathcal{Y}^{*J_1M_1}_{L_1S_1}(\hat{p}')\mathcal{Y}^{J'M'}_{L'S'}(\hat{p}')d\hat{p}' \rightarrow \langle L_1S_1J_1M_1|L'S'J'M'\rangle. \tag{2.79}$$

Inserting the bracket notation of the angular integration into expression (2.77) results in

$$\sum_{L_1S_1J_1M_1}\sum_{L'S'J'M'}\int A(\mathbf{p})\langle LSJM|L_1S_1J_1M_1\rangle V^1_{L_1}(p,p'). \tag{2.80}$$
$$\times\phi_{L'}(p')\langle L_1S_1J_1M_1|L'S'J'M'\rangle A(\mathbf{p}')p'^2dp'$$

Using the orthogonality condition

$$\langle LSJM|L'S'J'M'\rangle = \delta_{LL'}\delta_{SS'}\delta_{JJ'}\delta_{MM'} \tag{2.81}$$

the above equation becomes

$$\sum_{L_1S_1J_1M_1}\sum_{L'S'J'M'}\int A_1(\mathbf{p})A_2(\mathbf{p})\delta_{LL_1}\delta_{SS_1}\delta_{JJ_1}\delta_{MM_1}V^1_{L_1}(p,p') \tag{2.82}$$
$$\times\phi_{L'}(p')\delta_{L_1L'}\delta_{S_1S'}\delta_{J_1J'}\delta_{M_1M'}A_1(\mathbf{p}')A_2(\mathbf{p}')p'^2dp'.$$

After evaluating the delta functions we find

$$\int A_1(\mathbf{p})A_2(\mathbf{p})V^1_L(p,p')A_1(\mathbf{p}')A_2(\mathbf{p}')\phi_L(\hat{p}')p'^2dp'. \tag{2.83}$$

Since the first term of the effective potential contains no operations with spin dependent terms, we find that there is no coupling of angular momentum. In the next section we will calculate the matrix elements using the second term of the effective potential.

2.6.3 Effective Potential Term V^2 and V^3

In this section we will calculate the matrix elements of equation (2.75) using the second term of the effective potential V^2 in equation (2.76). The right hand side of equation (2.75) using V^2 is given by

$$\sum_{L_1S_1J_1M_1}\sum_{L'S'J'M'}\int \mathcal{Y}^{*JM}_{LS}(\hat{p})(\boldsymbol{\sigma}_1\cdot\mathbf{p})V^2_{L_1}(p,p')\mathcal{Y}^{J_1M_1}_{L_1S_1}(\hat{p})\mathcal{Y}^{*J_1M_1}_{L_1S_1}(\hat{p}') \tag{2.84}$$
$$\times(\boldsymbol{\sigma}_1\cdot\mathbf{p}')\phi'_L(p')\mathcal{Y}^{J'M'}_{L'S'}(\hat{p}')A_1(\mathbf{p})A_2(\mathbf{p})A_1(\mathbf{p}')A_2(\mathbf{p}')p'^2dp'd\hat{p}'d\hat{p}.$$

which, by using the bracket notation over the angular integration, we may write as

$$\sum_{L_1S_1J_1M_1}\sum_{L'S'J'M'}\int A_1(\mathbf{p})A_2(\mathbf{p})\langle LSJM|(\boldsymbol{\sigma}_1\cdot\mathbf{p})|L_1S_1J_1M_1\rangle V^2_{L_1}(p,p') \times\langle L_1S_1J_1M_1|(\boldsymbol{\sigma}_1\cdot\mathbf{p}')|L'S'J'M'\rangle\phi_{L'}(p')A_1(\mathbf{p}')A_2(\mathbf{p}')p'^2dp'. \tag{2.85}$$

In order to calculate the two matrix elements above, we will use the Wigner-Eckart theorem. The Wigner Eckart theorem for a tensor T^k_q of order k with $q=2k+1$ components is given by [22]

$$\langle jm|T^{(k)}_q|j'm'\rangle=\frac{1}{\sqrt{2j+1}}\langle j'km'q|j'kjm\rangle\langle j||\mathbf{T}^{(k)}||j'\rangle, \tag{2.86}$$

where $\langle j||\mathbf{T}^{(k)}||j'\rangle$ is the reduced matrix element. To calculate the reduced matrix element of the product of two vectors we use [22]

$$\langle j_1j_2jm|\mathbf{A}\cdot\mathbf{B}|j'_1j'_2j'm'\rangle=\delta_{jj'}\delta_{mm'}\langle j_1||\mathbf{A}||j'_1\rangle\langle j_2||\mathbf{B}||j'_2\rangle \times W(j_1j'_1j_2j'_2;1j)(-1)^{j'_2+j_1-j}, \tag{2.87}$$

where $W(j_1j'_1j_2j'_2;1j)$ are known as the Racah coefficients and are related to the 6-j symbols [23, 24]. We briefly discuss the Racah coefficients and the Clebsch-Gordan coefficients in Appendix C. We define an operator $\boldsymbol{\Sigma}=\frac{1}{2}(\boldsymbol{\sigma}_1-\boldsymbol{\sigma}_2)$. We also know that $\mathbf{S}=\frac{1}{2}(\boldsymbol{\sigma}_1+\boldsymbol{\sigma}_2)$, where $\boldsymbol{\sigma}_1$ and $\boldsymbol{\sigma}_2$ are the three-vector Pauli spin matrices for particle one and particle two. Using $\mathbf{S}$ and our definition of $\boldsymbol{\Sigma}$ we may write the first matrix element of equation as (2.85) as

$$\langle LSJM|(\boldsymbol{\Sigma}\cdot\mathbf{p}+\mathbf{S}\cdot\mathbf{p})|L_1S_1J_1M_1\rangle. \tag{2.88}$$

Using the Wigner-Eckart theorem for the scalar product of two tensors and noting that $\mathbf{p}=p\hat{p}$

$$\langle LSJM|\boldsymbol{\Sigma}\cdot\hat{p}|L_1S_1J_1M_1\rangle=\delta_{JJ_1}\delta_{MM_1}\langle L||\hat{p}||L_1\rangle\langle S||\boldsymbol{\Sigma}|S_1\rangle \times W(L_1S_1LS;J1)(-1)^{S_1+L+J} \tag{2.89}$$

and likewise we find

$$\langle LSJM|\mathbf{S}\cdot\hat{p}|L_1S_1J_1M_1\rangle=\delta_{JJ_1}\delta_{MM_1}\langle L||\hat{p}||L_1\rangle\langle S||\mathbf{S}|S_1\rangle \times W(L_1S_1LS;J1)(-1)^{S_1+L+J}. \tag{2.90}$$

The reduced matrix elements are found to be [25]

$$\begin{aligned}\langle S||\mathbf{S}||S_1\rangle &= \sqrt{S_1(S_1+1)(2S_1+1)}\delta_{SS_1}\\ \langle S||\boldsymbol{\Sigma}||S_1\rangle &= \sqrt{3}(-1)^{S+1}\delta_{S|S_1-1|}\\ \langle L||\hat{p}||L_1\rangle &= \langle L_1100|L0\rangle\sqrt{2L_1+1}.\end{aligned} \tag{2.91}$$

Thus for equation (2.88) we find

$$\begin{aligned}&\langle LSJM|(\boldsymbol{\Sigma}\cdot\mathbf{p}+\mathbf{S}\cdot\mathbf{p})|L_1S_1J_1M_1\rangle = \\ &\quad p\delta_{JJ_1}\delta_{MM_1}\sqrt{2L_1+1}\langle L_11;00|L0\rangle W(L_1S_1LS;J1)(-1)^{S_1+L+J}\\ &\quad\times\left[\sqrt{S(S+1)(2S+1)}\delta_{SS_1}+\sqrt{3}(-1)^{S+1}\delta_{S|S_1-1|}\right].\end{aligned} \tag{2.92}$$

We will find a similar expression for the second matrix element of equation (2.85)

$$\begin{aligned}\langle L_1 S_1 J_1 M_1|(\boldsymbol{\Sigma}\cdot\mathbf{p}+\mathbf{S}\cdot\mathbf{p})|L'S'J'M'\rangle = \\ p\delta_{J_1J'}\delta_{M_1M'}\sqrt{2L'+1}\langle L'1;00|L_10\rangle W(L'S'L_1S_1;J_11)(-1)^{S'+L_1+J_1} \\ \times\left[\sqrt{S_1(S_1+1)(2S_1+1)}\delta_{S'S_1}+\sqrt{3}(-1)^{S_1+1}\delta_{S_1|S'-1|}\right].\end{aligned} \tag{2.93}$$

Using the results from equations (2.92) and (2.93) we find that equation (2.85) becomes

$$\begin{aligned}\sum_{L_1S_1J_1M_1}\sum_{L'S'J'M'}\int A_1(\mathbf{p})A_2(\mathbf{p})\delta_{JJ_1} \\ \times\delta_{MM_1}\delta_{J_1J'}\delta_{M_1M'}\sqrt{2L_1+1}\sqrt{2L'+1} \\ \times\langle L_11;00|L0\rangle\langle L'1;00|L_10\rangle W(L_1S_1LS;J1)W(L'S'L_1S_1;J_11) \\ (-1)^{S_1+S'+L+L_1+J+J_1}\times \\ \Big[\sqrt{S(S+1)(2S+1)}\sqrt{S_1(S_1+1)(2S_1+1)}\delta_{SS_1}\delta_{S_1S'} \\ +\sqrt{S(S+1)(2S+1)}(-1)^{S_1+1}\sqrt{3}\delta_{S_1|S'-1|}\delta_{SS_1} \\ +\sqrt{S_1(S_1+1)(2S_1+1)}(-1)^{S+1}\sqrt{3}\delta_{S|S_1-1|}\delta_{S_1S'} \\ +3(-1)^{S+S_1+2}\delta_{S|S_1-1|}\delta_{S_1|S'-1|}\Big]V_{L_1}^2(p,p')\phi_{L'}(p')pp'p'^2dp'A_1(\mathbf{p}')A_2(\mathbf{p}').\end{aligned} \tag{2.94}$$

The next step is to evaluate the delta functions. This results in

$$\begin{aligned}\sum_{L_1L'}\int A_1(\mathbf{p})A_2(\mathbf{p})\langle L_11;00|L0\rangle\langle L'1;00|L_10\rangle V_{L_1}^2(p,p') \\ \times\quad\sqrt{2L_1+1}\sqrt{2L'+1} \\ \Big[S(S+1)(2S+1)W(L_1SLS;J1)W(L'SL_1S;J1)(-1)^{2S+L+L_1+2J} \\ +\sqrt{S(S+1)(2S+1)}(-1)^{S+1}\sqrt{3}W(L_1SLS;J1)W(L'|S-1|L_1S;J1) \\ \times(-1)^{S+|S-1|+L+L_1+2J} \\ +\sqrt{|S-1|(|S-1|+1)(2|S-1|+1)}(-1)^{S+1}\sqrt{3}W(L_1|S-1|LS;J1) \\ \times W(L'|S-1|L_1|S-1|;J1)(-1)^{|S-1|+|S-1|+L+L_1+2J} \\ +3(-1)^{S+|S-1|+2}W(L_1|S-1|LS;J1)W(L'SL_1|S-1|;J1) \\ \times(-1)^{|S-1|+S+L+L_1+2J}\Big]\phi_{L'}(p')pp'p'^2dp'A_1(\mathbf{p}')A_2(\mathbf{p}').\end{aligned} \tag{2.95}$$

We can use the two Clebsch-Gordan coefficients to rewrite L' in terms of L. The conditions that must be satisfied such that the Clebsch-Gordan coefficients are not zero is given by $L'+1-L_1=$ even and $L_1+1-L=$ even. These two conditions lead us to $L'=L+n$ where n is an even integer. However we find that either the Clebsch-Gordan or the Racah coefficients will vanish unless $n=0$. Therefore, the right hand side of equation (2.75) using the second term

of the effective potential V^2 in equation (2.76) is given by

$$\sum_{L_1}\int A_1(\mathbf{p})A_2(\mathbf{p})\langle L_1 1;00|L0\rangle\langle L1;00|L_1 0\rangle V^2_{L_1}(p,p') \tag{2.96}$$
$$\times \quad \sqrt{2L_1+1}\sqrt{2L+1}$$
$$\Big[S(S+1)(2S+1)W(L_1SLS;J1)W(LSL_1S;J1)(-1)^{2S+L+L_1+2J}$$
$$+\sqrt{S(S+1)(2S+1)}(-1)^{S+1}\sqrt{3}W(L_1SLS;J1)W(L|S-1|L_1S;J1)$$
$$\times(-1)^{S+|S-1|+L+L_1+2J}$$
$$+\sqrt{|S-1|(|S-1|+1)(2|S-1|+1)}(-1)^{S+1}\sqrt{3}W(L_1|S-1|LS;J1)$$
$$\times W(L|S-1|L_1|S-1|;J1)(-1)^{|S-1|+|S-1|+L+L_1+2J}$$
$$+3(-1)^{S+|S-1|+2}W(L_1|S-1|LS;J1)W(LSL_1|S-1|;J1)$$
$$\times(-1)^{|S-1|+S+L+L_1+2J}\Big]\phi_L(p')pp'p'^2dp'A_1(\mathbf{p}')A_2(\mathbf{p}').$$

The V^3 term is similar to the V^2 term. Using $\mathbf{S}=\frac{1}{2}(\boldsymbol{\sigma}_1+\boldsymbol{\sigma}_2)$ and our definition of $\boldsymbol{\Sigma}=\frac{1}{2}(\boldsymbol{\sigma_1}-\boldsymbol{\sigma_2})$, we can write $\boldsymbol{\sigma}_2=\mathbf{S}-\boldsymbol{\Sigma}$. Therefore the result for this term will be similar to equation (2.96) with the difference being in the phase factors and $V^3_{L_1}$. Hence, the right hand side of equation (2.75) using the third term of the effective potential V^3 from equation (2.76) is determined to be

$$\sum_{L_1}\int A_1(\mathbf{p})A_2(\mathbf{p})\langle L_1 1;00|L0\rangle\langle L1;00|L_1 0\rangle V^3_{L_1}(p,p') \tag{2.97}$$
$$\times \quad \sqrt{2L_1+1}\sqrt{2L+1}$$
$$\Big[S(S+1)(2S+1)W(L_1SLS;J1)W(LSL_1S;J1)(-1)^{2S+L+L_1+2J}$$
$$-\sqrt{S(S+1)(2S+1)}(-1)^{S+1}\sqrt{3}W(L_1SLS;J1)W(L|S-1|L_1S;J1)$$
$$\times(-1)^{S+|S-1|+L+L_1+2J}$$
$$-\sqrt{|S-1|(|S-1|+1)(2|S-1|+1)}(-1)^{S+1}\sqrt{3}W(L_1|S-1|LS;J1)$$
$$\times W(L|S-1|L_1|S-1|;J1)(-1)^{|S-1|+|S-1|+L+L_1+2J}$$
$$+3(-1)^{S+|S-1|+2}W(L_1|S-1|LS;J1)W(LSL_1|S-1|;J1)$$
$$\times(-1)^{|S-1|+S+L+L_1+2J}\Big]\phi_L(p')pp'p'^2dp'A_1(\mathbf{p}')A_2(\mathbf{p}').$$

Thus far, we have calculated the matrix elements of the Sucher equation using the first three terms of the effective potential. Next we will calculate the matrix element of the Sucher equation using the fourth term of the effective potential.

2.6.4 Effective Potential Term V^4

In this section, we will calculate the matrix element of equation (2.75) using the fourth term of the effective potential V^4 in equation (2.76). Using the fourth term of the effective potential, the

right hand side of equation (2.75) is given as

$$\sum_{L_1S_1J_1M_1}\sum_{L'S'J'M'}\int \mathcal{Y}^{*JM}_{LS}(\hat{p})(\boldsymbol{\sigma}_1\cdot\mathbf{p})(\boldsymbol{\sigma}_2\cdot\mathbf{p})V^4_{L_1}(p,p')\mathcal{Y}^{J_1M_1}_{L_1S_1}(\hat{p}) \tag{2.98}$$
$$\mathcal{Y}^{*J_1M_1}_{L_1S_1}(\hat{p}')(\boldsymbol{\sigma}_1\cdot\mathbf{p}')(\boldsymbol{\sigma}_2\cdot\mathbf{p}')\phi_{L'}(p')\mathcal{Y}^{J'M'}_{L'S'}(\hat{p}')d\mathbf{p}'d\mathbf{p}A_1(\mathbf{p})A_2(\mathbf{p})A_1(\mathbf{p}')A_2(\mathbf{p}').$$

Again we employ the bracket notation for the angular integration which results in

$$\sum_{L_1S_1J_1M_1}\sum_{L'S'J'M'}\int_0^\infty A_1(\mathbf{p})A_2(\mathbf{p})\langle LSJM|(\boldsymbol{\sigma}_1\cdot\hat{p})(\boldsymbol{\sigma}_2\cdot\hat{p})|L_1S_1J_1M_1\rangle \tag{2.99}$$
$$V^4_{L_1}(p,p')\langle L_1S_1J_1M_1|(\boldsymbol{\sigma}_1\cdot\hat{p}')(\boldsymbol{\sigma}_2\cdot\hat{p}')|L'S'J'M'\rangle\phi_{L'}(p')p^2p'^4dp'A_1(\mathbf{p}')A_2(\mathbf{p}').$$

The next task will be evaluating the matrix elements in the following expression

$$\sum_{L_1S_1J_1M_1}\sum_{L'S'J'M'}\langle LSJM|(\boldsymbol{\sigma}_1\cdot\hat{p})(\boldsymbol{\sigma}_2\cdot\hat{p})|L_1S_1J_1M_1\rangle \tag{2.100}$$
$$\times\langle L_1S_1J_1M_1|(\boldsymbol{\sigma}_1\cdot\hat{p})(\boldsymbol{\sigma}_2\cdot\hat{p})|L'S'J'M'\rangle V^4_{L_1}(p,p')\phi_{L'}(p').$$

To aid in calculation of the matrix element we will use the tensor operator. The tensor operate couples states of angular momentum with the same parity and is given by

$$\hat{S}_{12}=3(\boldsymbol{\sigma}_1\cdot\hat{u})(\boldsymbol{\sigma}_2\cdot\hat{u})-\boldsymbol{\sigma}_1\cdot\boldsymbol{\sigma}_2, \tag{2.101}$$

where $\hat{u}$ is an arbitrary unit vector. We use this to write

$$(\boldsymbol{\sigma}_1\cdot\hat{u})(\boldsymbol{\sigma}_2\cdot\hat{u})=\frac{1}{3}\left[\hat{S}_{12}(\hat{u})+\boldsymbol{\sigma}_1\cdot\boldsymbol{\sigma}_2\right]. \tag{2.102}$$

Thus equation (2.100) becomes

$$\frac{1}{9}\sum_{L_1S_1J_1M_1}\sum_{L'S'J'M'}\langle LSJM|(\hat{S}_{12}+\boldsymbol{\sigma}_1\cdot\boldsymbol{\sigma}_2)|L_1S_1J_1M_1\rangle \tag{2.103}$$
$$\times\langle L_1S_1J_1M_1|(\hat{S}_{12}+\boldsymbol{\sigma}_1\cdot\boldsymbol{\sigma}_2)|L'S'J'M'\rangle V^4_{L_1}(p,p')\phi_{L'}(p').$$

We know how the tensor operator and $\boldsymbol{\sigma}_1\cdot\boldsymbol{\sigma}_2$ act on singlet and triplet states. Note that

$$[\boldsymbol{\sigma}_1\cdot\boldsymbol{\sigma}_2]|SM_S\rangle=[S(S+1)-3]|SM_S\rangle. \tag{2.104}$$

So for the singlet state ($S=0$), $\boldsymbol{\sigma}_1\cdot\boldsymbol{\sigma}_2=-3$ and for triplet states ($S=1$), $\boldsymbol{\sigma}_1\cdot\boldsymbol{\sigma}_2=1$. When the tensor operator acts on singlet states, then

$$\hat{S}_{12}\mathcal{Y}^{JM}_{L0}=0. \tag{2.105}$$

The tensor operator acts on triplet states in the following way [26]

$$\begin{aligned}
\hat{S}_{12}\mathcal{Y}^{JM}_{J1} &= 2\mathcal{Y}^{JM}_{LS} \quad \text{for L = J} \\
\hat{S}_{12}\mathcal{Y}^{JM}_{J+11} &= \alpha\mathcal{Y}^{JM}_{J+1S}+\beta\mathcal{Y}^{JM}_{J-1S} \quad \text{for L = J+1} \\
\hat{S}_{12}\mathcal{Y}^{JM}_{J-11} &= \gamma\mathcal{Y}^{JM}_{J+1S}+\kappa\mathcal{Y}^{JM}_{J-1S} \quad \text{for L = J-1,}
\end{aligned} \tag{2.106}$$

where

$$\alpha = \frac{6J}{2J+1} - 4 \qquad \beta = \frac{6\sqrt{J(J+1)}}{2J+1} \tag{2.107}$$
$$\gamma = \frac{6\sqrt{J(J+1)}}{2J+1} \qquad \kappa = \frac{6(J+1)}{2J+1} - 4.$$

Now we will calculate the matrix elements of (2.100) using our knowledge of how the tensor operator acts on singlet and triplet states. There is one singlet state to consider with $S = 0$ and three triplet states to consider with $S = 1$ and $L = J$, $L = J+1$, and $L = J-1$.

2.6.5 Singlet State

For the singlet state, expression (2.100) becomes

$$\frac{1}{9}\sum_{L_1S_1J_1M_1}\sum_{L'S'J'M'}\langle L0JM|(\hat{S}_{12}+\boldsymbol{\sigma}_1\cdot\boldsymbol{\sigma}_2)|L_1S_1J_1M_1\rangle V^4_{L_1}\phi_{L'} \\ \times\langle L_1S_1J_1M_1|(\hat{S}_{12}+\boldsymbol{\sigma}_1\cdot\boldsymbol{\sigma}_2)|L'S'J'M'\rangle\phi_{L'}(p'), \tag{2.108}$$

where we have used the definition of the the tensor operator to rewrite the matrix elements as in equation (2.102). Next we use $S_{12} = 0$ and $\boldsymbol{\sigma}_1\cdot\boldsymbol{\sigma}_2 = -3$ to evaluate the first matrix element resulting in

$$-\frac{1}{3}\sum_{L_1S_1J_1M_1}\sum_{L'S'J'M'}\langle L_1S_1J_1M_1|(\hat{S}_{12}+\boldsymbol{\sigma}_1\cdot\boldsymbol{\sigma}_2)|L'S'J'M'\rangle \\ \times V^4_L\phi_{L'}\delta_{L_1L}\delta_{S_10}\delta_{J_1J}\delta_{M_1M}. \tag{2.109}$$

We repeat this process for the second matrix element

$$= -\frac{1}{3}\sum_{L'S'J'M'}\langle L0JM|(\hat{S}_{12}+\sigma_1\cdot\sigma_2)|L'S'J'M'\rangle V^4_L\phi_{L'} \\ = V^4_L(p,p')\phi_L(p'). \tag{2.110}$$

We note that, as expected, there is no angular momentum coupling with the singlet state. Next we calculate the matrix element of the $L = J$ triplet state.

2.6.6 Triplet State L=J

In this section we will calculate the matrix elements in equation (2.100) of the $L = J$ triplet State.

$$\frac{1}{9}\sum_{L_1S_1J_1M_1}\sum_{L'S'J'M'}\langle J1JM|(\hat{S}_{12}+\boldsymbol{\sigma}_1\cdot\boldsymbol{\sigma}_2)|L_1S_1J_1M_1\rangle \\ \times\langle L_1S_1J_1M_1|(\hat{S}_{12}+\boldsymbol{\sigma}_1\cdot\boldsymbol{\sigma}_2)|L'S'J'M'\rangle V^4_{L_1}\phi_{L'}$$

Using our knowledge of how the triplet state operates on the vector spherical harmonics from equation (2.106) and $\boldsymbol{\sigma}_1 \cdot \boldsymbol{\sigma}_2 = 1$, we write equation the above equation as

$$\begin{aligned}\frac{1}{3}\sum_{L_1S_1J_1M_1}\sum_{L'S'J'M'}\delta_{L_1J}\delta_{S_11}\delta_{J_1J}\delta_{M_1M}\langle L_1S_1J_1M_1|(\hat{S}_{12}+\boldsymbol{\sigma}_1\cdot\boldsymbol{\sigma}_2)|L'S'J'M'\rangle V^4_{L_1}\phi_{L'}&\\ = \frac{1}{3}\sum_{L'S'J'M'}\langle J1JM|(\hat{S}_{12}+\boldsymbol{\sigma}_1\cdot\boldsymbol{\sigma}_2)|L'S'J'M'\rangle V^4_{L_1}\phi_{L'}&\\ = V^4_J(p,p')\phi_J(p'). \qquad (2.111)\end{aligned}$$

We have shown that there is no coupling of angular momentum for the $L = J$ triplet state. Next we calculate the matrix elements for the $L = J+1$ triplet state.

2.6.7 Triplet States $L = J+1$ and $L = J-1$

In this section, we will calculate the matrix elements (2.100) for the $L = J+1$ triplet state.

$$\begin{aligned}\frac{1}{9}\sum_{L_1S_1J_1M_1}\sum_{L'S'J'M'}\langle J+1\,1JM|(\hat{S}_{12}+\boldsymbol{\sigma}_1\cdot\boldsymbol{\sigma}_2)|L_1S_1J_1M_1\rangle \qquad (2.112)\\ \times\langle L_1S_1J_1M_1|(\hat{S}_{12}+\boldsymbol{\sigma}_1\cdot\boldsymbol{\sigma}_2)|L'S'J'M'\rangle V^4_{L_1}(p,p')\phi_{L'}(p')\end{aligned}$$

Again we utilize equation (2.106) and $\boldsymbol{\sigma}_1 \cdot \boldsymbol{\sigma}_2 = 1$ to write the above expression as

$$\begin{aligned}\frac{1}{9}\sum_{L_1S_1J_1M_1}\sum_{L'S'J'M'}\left[(\alpha+1)\delta_{L_1J+1}+\beta\delta_{L_1J-1}\right]&\\ \times\delta_{S_11}\delta_{J_1J}\delta_{M_1M}V^4_{L_1}(p,p')\phi_{L'}(p')&\\ \times\langle L_1S_1J_1M_1|(\hat{S}_{12}+\boldsymbol{\sigma}_1\cdot\boldsymbol{\sigma}_2)|L'S'J'M'\rangle V_{L_1}(p,p')\phi_{L'}(p').&\end{aligned}$$

Next we evaluate the second matrix element

$$\begin{aligned}\frac{1}{9}\sum_{L'S'J'M'}\Bigg[(\alpha+1)V^4_{J+1}(p,p')\Big((\alpha+1)\delta_{L'J+1}+\beta\delta_{L'J-1}\Big)\phi_{L'}(p')&\\ \times\delta_{S'1}\delta_{J'J}\delta_{M'M}&\\ +\beta V^4_{J-1}(p,p')\Big(\gamma\delta_{L'J+1}+\kappa\delta_{l'J-1}\Big)\phi_{L'}(p')\delta_{S'1}\delta_{J'J}\delta_{M'M}\Bigg].&\end{aligned}$$

Finally we evaluate the delta functions, and for the $L = J+1$ triplet state, equation (2.100) becomes

$$\begin{aligned}\frac{1}{9}\Big[(\alpha+1)^2V^4_{J+1}(p,p')+\beta\gamma V^4_{J-1}(p,p')\Big]\phi_{J+1}(p') \qquad (2.113)\\ +\frac{1}{9}\Big[(\alpha+1)\beta V^4_{J+1}(p,p')+(\kappa+1)\beta V^4_{J-1}(p,p')\Big]\phi_{J-1}(p').\end{aligned}$$

This result shows that the $L = J+1$ and $L = J-1$ states are coupled. If we follow the same steps as we did for the $L = J+1$ triplet state, we find that for the $L = J-1$ equation (2.100) is

given by

$$= \frac{1}{9}\Big[\gamma(\alpha+1)V^4_{J+1}(p,p') + \gamma(\kappa+1)V_{J-1}(p,p')\Big]\phi_{J+1}(p') \tag{2.114}$$
$$+\frac{1}{9}\Big[(\gamma\beta V^4_{J+1}(p,p') + (\kappa+1)^2 V_{J-1}(p,p')\Big]\phi_{J-1}(p').$$

Again, our results show that the $L = J+1$ and $L = J-1$ states are coupled.

2.6.8 Singlet and Triplet Results for V^4 term

The results for the singlet and triplet state matrix elements are listed in this section. For the singlet state, expression (2.99) becomes

$$\int A_1(\mathbf{p})A_2(\mathbf{p})V^4_L(p,p')\phi_L(p')p^2p'^4dp'A_1(\mathbf{p}')A_2(\mathbf{p}'). \tag{2.115}$$

For the triplet state with $L = J$, expression (2.99) is given by

$$\int A_1(\mathbf{p})A_2(\mathbf{p})V^4_J(p,p')\phi_J(p')p^2p'^4dp'A_1(\mathbf{p}')A_2(\mathbf{p}'). \tag{2.116}$$

For the triplet state with $L = J+1$, expression (2.99) is given by

$$\frac{1}{9}\int\Bigg[\Big((\alpha+1)^2V^4_{J+1}(p,p') + \beta\gamma V^4_{J-1}(p,p')\Big)\phi_{J+1}(p') \tag{2.117}$$
$$+\Big(\beta(\alpha+1)V^4_{J+1}(p,p') + \beta(\kappa+1)V^4_{J-1}(p,p')\Big)\phi_{J-1}(p')\Bigg]$$
$$\times p^2p'^4dp'A_1(\mathbf{p})A_2(\mathbf{p})A_1(\mathbf{p}')A_2(\mathbf{p}').$$

For the triplet state with $L = J-1$, expression (2.99) is given by

$$\frac{1}{9}\int\Bigg[\Big(\gamma(\alpha+1)V^4_{J+1}(p,p') + \gamma(\kappa+1)V^4_{J-1}(p,p')\Big)\phi_{J+1}(p') \tag{2.118}$$
$$+\Big(\gamma\beta V^4_{J+1}(p,p') + (\kappa+1)^2V^4_{J-1}(p,p')\Big)\phi_{J-1}(p')\Bigg]$$
$$\times p^2p'^4dp'A_1(\mathbf{p})A_2(\mathbf{p})A_1(\mathbf{p}')A_2(\mathbf{p}').$$

We can see from the calculations above that the result of V^4 is to couple angular momentum for the $L = J\pm1$ triplet states. As expected, there is no coupling for the singlet state or the $L = J$ triplet state.

2.7 Final Results for Sucher Equation

At this stage we have computed the matrix elements for each term of the effective potential. All that remains is to write the Sucher equation for the singlet state and triplet states. This entails evaluating the Clebsch-Gordan coefficients and the Racah coefficient at $S = 0$ for the singlet states and $S = 1$ for the triplet states. In addition, we must substitute $L = J$, $L = J+1$, or $L = J-1$ for the triplet states.

2.7.1 Singlet State Sucher Equation

We now combine all of the results for the each term of the effective potential into one equation for the singlet state. For $S = 0$ the Sucher equation is

$$
\begin{aligned}
&\big[\sqrt{p^2+m_1^2}+\sqrt{p^2+m_2^2}\big]\,\phi_L(p) \\
&+\int A_1(\mathbf{p})A_2(\mathbf{p})V_L^1(p,p')A_1(\mathbf{p}')A_2(\mathbf{p}')\phi_L(p')p'^2dp' \\
&+\sum_{L_1}(-1)^{L_1+L}\int A_1(\mathbf{p})A_2(\mathbf{p})\langle L_1 1;00|L0\rangle\langle L\,1;00|L_1 0\rangle V_{L_1}^2(p,p') \\
&\times\sqrt{2L_1+1}\sqrt{2L+1} \\
&\Big[-3\sqrt{2}W(L_1\,1\,L0;J\,1)W(L\,1\,L_1\,1;J\,1) \\
&+3W(L_1\,1\,L0;J\,1)W(L0\,L_1\,1;J\,1)\Big]\phi_L(p')pp'p'^2dp'A_1(\mathbf{p}')A_2(\mathbf{p}') \\
&+\sum_{L_1}(-1)^{L_1+L}\int A_1(\mathbf{p})A_2(\mathbf{p})\langle L_1 1;00|L0\rangle\langle L\,1;00|L_1 0\rangle V_{L_1}^3(p,p') \\
&\times\sqrt{2L_1+1}\sqrt{2L+1} \\
&\Big[3\sqrt{2}W(L_1\,1\,L0;J\,1)W(L\,1\,L_1\,1;J\,1) \\
&+3W(L_1\,1\,L0;J\,1)W(L0\,L_1\,1;J\,1)\Big]\phi_L(p')pp'p'^2dp'A_1(\mathbf{p}')A_2(\mathbf{p}') \\
&+\int A_1(\mathbf{p})A_2(\mathbf{p})V_L^4(p,p')\phi_L(p')p^2p'^4dp'A_1(\mathbf{p}')A_2(\mathbf{p}') = E\phi_L(p).
\end{aligned}
\tag{2.119}
$$

2.7.2 Triplet State Sucher Equation ($L = J$)

The Sucher equation for the triplet state with $L = J$ and $S = 1$ is given by

$$
\begin{aligned}
&\big[\sqrt{p^2+m_1^2}+\sqrt{p^2+m_2^2}\big]\phi_J(p) \\
&+\int A_1(\mathbf{p})A_2(\mathbf{p})V_J^1(p,p')A_1(\mathbf{p}')A_2(\mathbf{p}')\phi_J(p')p'^2dp' \\
&+\sum_{L_1}\int A_1(\mathbf{p})A_2(\mathbf{p})\langle L_1 1;00|J0\rangle\langle J\,1;00|L_1 0\rangle V_{L_1}^2(p,p') \\
&\times(-1)^{L_1+J}\sqrt{2L_1+1}\sqrt{2J+1} \\
&\times\Big[6W(L_1\,1\,J\,1;J\,1)W(J\,1\,L_1\,1;J\,1) \\
&-3\sqrt{2}W(L_1\,1\,J\,1;J\,1)W(J\,0\,L_1\,1;J\,1) \\
&+3W(L_1\,0\,J\,1;J\,1)W(J\,1\,L_1\,0;J\,1)\Big]\phi_J(p')pp'p'^2dp'A_1(\mathbf{p}')A_2(\mathbf{p}') \\
&+\sum_{L_1}\int A_1(\mathbf{p})A_2(\mathbf{p})\langle L_1 1;00|J0\rangle\langle J\,1;00|L_1 0\rangle V_{L_1}^3(p,p') \\
&\times(-1)^{L_1+J}\sqrt{2L_1+1}\sqrt{2J+1} \\
&\times\Big[6W(L_1\,1\,J\,1;J\,1)W(J\,1\,L_1\,1;J\,1) \\
&+3\sqrt{2}W(L_1\,1\,J\,1;J\,1)W(J\,0\,L_1\,1;J\,1) \\
&+3W(L_1\,0\,J\,1;J\,1)W(J\,1\,L_1\,0;J\,1)\Big]\phi_J(p')pp'p'^2dp'A_1(\mathbf{p}')A_2(\mathbf{p}') \\
&+\int A_1(\mathbf{p})A_2(\mathbf{p})V_J^4(p,p')\phi_J(p')p^2p'^4dp'A_1(\mathbf{p}')A_2(\mathbf{p}') = E\phi_J(p).
\end{aligned}
\tag{2.120}
$$

2.7.3 Triplet State Sucher Equation ($L = J+1$)

The Sucher equation for the triplet state with $L = J+1$ and $S = 1$ is given by the equation below. The angular momentum coupling can be seen in the $\phi_{J+1}(p')$ and $\phi_{J-1}(p')$ terms.

$$
\begin{aligned}
&\left[\sqrt{p^2+m_1^2}+\sqrt{p^2+m_2^2}\right]\phi_{J+1}(p) \\
&+\int V^1_{J+1}(p,p')A_1(\mathbf{p})A_2(\mathbf{p})A_1(\mathbf{p}')A_2(\mathbf{p}')\phi_{J+1}(p')p'^2dp' \\
&+\sum_{L_1}(-1)^{L_1+J+1}\int A_1(\mathbf{p})A_2(\mathbf{p})\langle L_1 1;00|J+10\rangle\langle J+1\,1;00|L_1 0\rangle V^2_{L_1}(p,p') \\
&\times\sqrt{2L_1+1}\sqrt{2(J+1)+1} \\
&\times\Bigg[6W(L_1\,1\,J+1\,1;J\,1)W(J+1\,1\,L_1\,1;J\,1) \\
&-3\sqrt{2}W(L_1\,1\,J+1\,1;J\,1)W(J+1\,0\,L_1\,1;J\,1) \\
&+3W(L_1\,0\,J+1\,1;J\,1)W(J+1\,1\,L_1\,0;J\,1)\Bigg]\phi_{J+1}(p')pp'p'^2dp'A_1(\mathbf{p}')A_2(\mathbf{p}') \\
&+\sum_{L_1}(-1)^{L_1+J+1}\int A_1(\mathbf{p})A_2(\mathbf{p})\langle L_1 1;00|J0\rangle\langle J+1\,1;00|L_1 0\rangle V^3_{L_1}(p,p') \\
&\times\sqrt{2L_1+1}\sqrt{2(J+1)+1} \\
&\times\Bigg[6W(L_1\,1\,J+1\,1;J\,1)W(J+1\,1\,L_1\,1;J\,1) \\
&+3\sqrt{2}W(L_1\,1\,J+1\,1;J\,1)W(J+1\,0\,L_1\,1;J\,1) \\
&+3W(L_1\,0\,J+1\,1;J\,1)W(J+1\,1\,L_1\,0;J\,1)\Bigg]\phi_{J+1}(p')pp'p'^2dp'A_1(\mathbf{p}')A_2(\mathbf{p}') \\
&\frac{1}{9}\int A_1(\mathbf{p})A_2(\mathbf{p})\Bigg[\Big((\alpha+1)^2V^4_{J+1}(p,p')+\beta\gamma V^4_{J-1}(p,p')\Big)\phi_{J+1}(p') \\
&+\Big(\beta(\alpha+1)V^4_{J+1}(p,p')+\beta(\kappa+1)V^4_{J-1}(p,p')\Big)\phi_{J-1}(p')\Bigg]p^2p'^4dp'A_1(\mathbf{p}')A_2(\mathbf{p}') \\
&=E\phi_{J+1}(p)
\end{aligned}
\tag{2.121}
$$

2.7.4 Triplet State Sucher Equation ($L = J-1$)

The Sucher equation for the triplet state with $L = J-1$ and $S = 1$ is given by the equation below. The angular momentum coupling is seen in the $\phi_{J+1}(p')$ and the $\phi_{J-1}(p')$ terms.

$$
\begin{aligned}
&\left[\sqrt{p^2+m_1^2}+\sqrt{p^2+m_2^2}\right]\phi_{J-1}(p) \\
&+\int A_1(\mathbf{p})A_2(\mathbf{p})V^1_{J-1}(p,p')A_1(\mathbf{p}')A_2(\mathbf{p}')\phi_{J-1}(p')p'^2dp' \\
&+\sum_{L_1}(-1)^{L_1+J-1}\int A_1(\mathbf{p})A_2(\mathbf{p})\langle L_1 1;00|J-10\rangle\langle J-1\,1;00|L_1 0\rangle V^2_{L_1}(p,p') \\
&\times\sqrt{2L_1+1}\sqrt{2(J-1)+1} \\
&\Big[6W(L_1\,1\,J-1\,1;J\,1)W(J-1\,1\,L_1\,1;J\,1) \\
&-3\sqrt{2}W(L_1\,1\,J-1\,1;J\,1)W(J-1\,0\,L_1\,1;J\,1) \\
&+3W(L_1\,0\,J-1\,1;J\,1)W(J-1\,1\,L_1\,0;J\,1)\Big]\phi_{J-1}(p')pp'p'^2dp'A_1(\mathbf{p}')A_2(\mathbf{p}') \\
&+\sum_{L_1}(-1)^{L_1+J-1}\int A_1(\mathbf{p})A_2(\mathbf{p})\langle L_1 1;00|J0\rangle\langle J-1\,1;00|L_1 0\rangle V^3_{L_1}(p,p') \\
&\times\sqrt{2L_1+1}\sqrt{2(J-1)+1} \\
&\Big[6W(L_1\,1\,J-1\,1;J\,1)W(J-1\,1\,L_1\,1;J\,1) \\
&+3\sqrt{2}W(L_1\,1\,J-1\,1;J\,1)W(J-1\,0\,L_1\,1;J\,1) \\
&+3W(L_1\,0\,J-1\,1;J\,1)W(J-1\,1\,L_1\,0;J\,1)\Big]\phi_{J-1}(p')pp'p'^2dp'A_1(\mathbf{p}')A_2(\mathbf{p}') \\
&\frac{1}{9}\int A_1(\mathbf{p})A_2(\mathbf{p})\Big[\Big(\gamma(\alpha+1)V^4_{J+1}(p,p')+\gamma(\kappa+1)V^4_{J-1}(p,p')\Big)\phi_{J+1}(p') \\
&+\Big(\gamma\beta V^4_{J+1}(p,p')+(\kappa+1)^2V^4_{J-1}(p,p')\Big)\phi_{J-1}(p')\Big]p^2p'^4dp'A_1(\mathbf{p}')A_2(\mathbf{p}') \\
&=E\phi_{J-1}(p)
\end{aligned}
\tag{2.122}
$$

Chapter 3

NUMERICAL METHODS AND POTENTIAL MODELS

3.1 Numerical Methods

In the last chapter we showed how to write the Schrödinger equation in the position space, mixed-space, and momentum space representations. We also derived the Sucher equation and showed how to compute the matrix elements. Finally we presented the lth partial wave for the singlet and triplet states. It was also shown that for a central potential, the Schrödinger equation in the position space, mixed space, and momentum space representations was uncoupled. The Sucher equation is also uncoupled for the singlet state and $L = J$ triplet state. In contrast, the Sucher equation is coupled for the $L = J \pm 1$ triplet states. In this section we discuss the numerical methods used to solve the Schrödinger equation and the Sucher equation.

We showed that the Schrödinger equation could be written as

$$\sum_j H_{ij} c_j = E c_i, \tag{3.1}$$

where H_{ij} is obtained by carrying out the integrals in equations (2.28), (2.40), and (2.45). We used Gaussian quadrature to carry out the integration. This is discussed in Appendix D. We also showed that we could represent equation (3.1) as a matrix equation

$$\tilde{H}\mathbf{c} = E\mathbf{c}. \tag{3.2}$$

Next this equation could be solved for the eigenvalues and eigenvectors. We associate the eigenvalues with energy, and we use the eigenvectors c_j to reconstruct the wave function. We expanded the wavefunctions in terms of a complete orthonormal basis set. This would entail using an infinite set of orthonormal basis functions. It is numerically impossible to use an infinite number of basis functions, thus we approximate this by a maximum number $N_{\max}$. The expansion of the position space wave function then takes the form

$$\psi_l(r) = \sum_{j=1}^{N_{\max}} g_j(r) c_j. \tag{3.3}$$

In such an approximation, the variational principle is used to calculate the upper bound of the ground state energy. We associate the higher eigenvalues with the excited energy states. A variational parameter is used to compensate for truncating the number of basis functions. The variational principle is discussed in Appendix A, and we discuss our choice of orthonormal basis functions in Appendix E.

The Schrödinger equation in the position space, mixed space, and momentum space representions, the singlet state Sucher equation, and $L = J$ triplet state Sucher equation may be expanded as in equation (3.3). As an example, let us consider $N_{max} = 2$ and construct our matrix equation. We can write equation (3.1) as a matrix equation

$$\begin{pmatrix} H_{11} & H_{12} \\ H_{21} & H_{22} \end{pmatrix} \begin{pmatrix} c_1 \\ c_2 \end{pmatrix} = E \begin{pmatrix} c_1 \\ c_2 \end{pmatrix}. \tag{3.4}$$

We can now solve for the eigenvalues and eigenvectors.

Next we examine the coupled Sucher equation. The $L = J+1$ and $L = J-1$ Sucher equations are coupled and cannot be solved in exactly the same way as the uncoupled equations. The coupled Sucher equations (2.121) and (2.122) have the structure

$$\begin{aligned} T(p)\phi_{J-1}(p) + \int_0^\infty A_1(p,p')\phi_{J-1}(p')dp' \\ + \int_0^\infty A_2(p,p')\phi_{J+1}(p')dp' = E\phi_{J-1}(p) \end{aligned} \tag{3.5}$$

$$\begin{aligned} T(p)\phi_{J+1}(p) + \int_0^\infty A_3(p,p')\phi_{J-1}(p')dp' \\ + \int_0^\infty A_4(p,p')\phi_{J+1}(p')dp' = E\phi_{J+1}(p), \end{aligned} \tag{3.6}$$

where the A's are known functions of p and p' In this case we will expand both $\phi_{J-1}(p)$ and $\phi_{J+1}(p)$ in terms of the momentum space basis described in Appendix E,

$$\phi_{J-1}(p) = \sum_{j=1}^{N_{\max}} g_j(p)c_j \quad \text{and} \quad \phi_{J+1}(p) = \sum_{j=1}^{N_{\max}} f_j(p)d_j, \tag{3.7}$$

where $f_j(p)$ and $g_j(p)$ are the functions and c_j and d_j are the coefficients. We substitute this in equations (3.5) and (3.6). Next we project from the left onto equation 3.5 with $f_i(p)p^2dp$ and we integrate over dp. Likewise, we project from the left onto equation 3.6 with $g_i(p)p^2dp$ and we integrate over dp giving us

$$\begin{aligned} \sum_{j=1}^{N_{\max}} \Bigg[\int_0^\infty T(p)g_i(p)g_j(p)p^2dp\, c_j \\ + \int_0^\infty A_1(p,p')g_i(p)g_j(p')p^2dp'dp\, c_j \\ + \int_0^\infty A_2(p,p')g_i(p)f_j(p')p^2dpdp'\, d_j \Bigg] = Ec_i \end{aligned} \tag{3.8}$$

$$\begin{aligned} \sum_{j=1}^{N_{\max}} \Bigg[\int_0^\infty T(p)f_i(p)f_j(p)p^2dp\, d_j \\ + \int_0^\infty A_3(p,p')f_i(p)g_j(p')p^2dp'dp\, c_j \\ + \int_0^\infty A_4(p,p')f_i(p)f_j(p')p^2dpdp'\, d_j \Bigg] = Ed_i, \end{aligned} \tag{3.9}$$

where we have used the orthonormality condition satisfied by $g_j(p)$ and $f_j(p)$ as described in Appendix E. Next we carry out the integration using Gaussian Quadrature (Appendix D). We group and relabel terms that multiply the coefficients:

$$\sum_{j=1}^{N_{\max}} B_{ij}c_j + C_{ij}d_j = Ec_i \tag{3.10}$$

$$\sum_{j=1}^{N_{\max}} D_{ij}c_j + F_{ij}d_j = Ed_i, \tag{3.11}$$

where

$$B_{ij} = \int_0^\infty T(p)g_i(p)g_j(p)p^2dp + \int_0^\infty A_1(p,p')g_i(p)g_j(p')p^2dp'dp \tag{3.12}$$

$$C_{ij} = \int_0^\infty A_2(p,p')g_i(p)f_j(p')p^2dpdp' \tag{3.13}$$

$$D_{ij} = \int_0^\infty A_3(p,p')f_i(p)g_j(p')p^2dpdp' \tag{3.14}$$

$$F_{ij} = \int_0^\infty T(p)f_i(p)f_j(p)p^2dp + \int_0^\infty A_4(p,p')f_i(p)f_j(p')p^2dpdp'. \tag{3.15}$$

Now we can take equations (3.10) and (3.11) and write them as a matrix equation

$$\begin{pmatrix} \mathbf{B} & \mathbf{C} \\ \mathbf{D} & \mathbf{F} \end{pmatrix} \begin{pmatrix} \mathbf{c} \\ \mathbf{d} \end{pmatrix} = E \begin{pmatrix} \mathbf{c} \\ \mathbf{d} \end{pmatrix}. \tag{3.16}$$

As an example, we will expand our basis functions with $N_{\max} = 2$ and the above equation becomes

$$\begin{pmatrix} B_{11} & B_{12} & C_{11} & C_{12} \\ B_{21} & B_{22} & C_{22} & C_{22} \\ D_{11} & D_{12} & F_{11} & F_{12} \\ D_{21} & D_{22} & F_{21} & F_{22} \end{pmatrix} \begin{pmatrix} c_1 \\ c_2 \\ d_1 \\ d_2 \end{pmatrix} = E \begin{pmatrix} c_1 \\ c_2 \\ d_1 \\ d_2 \end{pmatrix}. \tag{3.17}$$

Again we solve the eigenvalue problem to obtain the eigenvalues and eigenvectors. The energy is given by the eigenvalues and the eigenvectors c_j and d_j are used to reconstruct the wave functions in equation (3.7).

3.2 Potential Model

In Quantum Chromodynamics (QCD), quarks interact by exchanging gluons. Gluons are the force carrying particles of the strong force. Gluons carry color-charge, which means the may interact with quarks and with themselves. Figure (3.1) shows the flux tube model of the meson system. The lines represent the interaction of the quarks with the gluons and the self interaction of the gluons.

Phenomenological potentials have been used to model quark-antiquark and gluon interactions [27, 28, 29, 30, 31, 32, 33]. At short distances the mesons behave as essentially free particles. A one gluon exchange model (OGE) [34] is used for short range interaction and

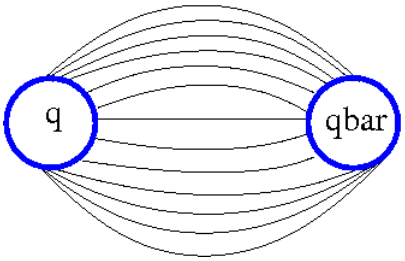

Figure 3.1: Flux tube diagram for a quarkonium system. The lines represent the interaction of the quarks with gluons and the self interaction of the gluons.

results in a Coulomb-like potential. Experimentally evidence has never revealed the existence of free quarks in nature. Therefore it is assumed that quarks exist only in color singlet bound states. In the quark model, mesons are bound states of quarks and anti-quarks. In order to study meson spectra using phenomenology, we need potentials to simulate quark confinement and asymptotic freedom. We use a linear potential to simulate the quark confinement. The exact form of this interaction cannot yet be derived. Thus our model of the potential has the form

$$V(r) = \frac{C}{r} + \sigma r, \tag{3.18}$$

where C is the coupling parameter for the OGE interaction, and σ is the coupling parameter for confinement. Our potential appears to be problematic at first, because the Coulomb-like potential and the linear potential are both singular in momentum space. However a substraction methods have been developed to deal with the singularities. The results of the subtraction method are discussed in Appendix F. Since the Sucher equation is in momentum space, we will need to verify that our momentum space program is functioning properly. The Schrödinger equation will yield the same results regardless of whether it is derived in position space, mixed-space, or momentum space. If we consider the Schrödinger equation with non-relativistic kinematics with a purely linear potential and $l = 0$, we can show that the position space Schrödinger equation may be written as the Airy differential equation. The energies are related to the roots of the Airy function x_n, by

$$E_{n-1} = \left(\frac{\sigma^2}{2\mu}\right)^{\frac{1}{3}} |x_n|. \tag{3.19}$$

The ground state energy E_0 is proportional to the first root of the Airy function x_1. Likewise the excited states are proportional to the higher roots of the Airy function. In table (3.1), we use a linear potential with $l = 0$ and $\sigma = 1$ GeV^2, and $\mu = 0.5$ GeV to solve the non-relativistic momentum space Schrödinger equation for the energy. The momentum space results are in exact agreement with the roots of the Airy function [1]. Next we can use a purely Coulomb potential with $l = 0$ to verify our momentum space results. We can scale the momentum space Schrödinger equation (2.23) such that it is dimensionless and the bound state energy is given by $E = Z^2/2n^2$, where Z is the atomic number. The result of this work has been published by Werneth et. al. [35]. We show in table (3.2) that the results of the non-relativistic momentum

Table 3.1: Non-relativistic Momentum-space Results for Purely Linear Potential with $l = 0$, $\sigma = 1$ GeV^2, and $\mu = 0.5$ GeV. The Energies are in Exact Agreement with the Roots of the Airy Function as Given by Abramowitz and Stegun [1].

E_n	p-space (NR)	Roots of Airy's Function [1]
E_0	2.33810741	2.33810741
E_1	4.08794944	4.08794944
E_2	5.52055983	5.52055983
E_3	6.78670809	6.78670809
E_4	7.94413359	7.94413359

Table 3.2: Non-relativistic Momentum-space Results for Purely Coulomb Potential with $l = 0$ and $Z = 1$ ($C = 1$). The Bound State Energy is Given by $E = Z^2/2n^2$.

E_n	p-space (NR)	Expected Energy
E_1	0.50000000	0.50000000
E_2	0.12500000	0.12500000
E_3	0.05555556	0.05555556
E_4	0.06250000	0.06250000
E_5	0.04000000	0.04000000

space Schrödinger equation with a purely Coulomb potential with $l = 0$ and $Z = 1$ ($C = 1$) gives us the expected bound state energy. In both cases, 60 Jacobi basis functions were used for the calculations. These two calculations verify that our momentum space program is working correctly.

Our goal in this thesis is to use the Sucher equation for $c\bar{c}$ and $b\bar{b}$ spectroscopy. For our first approximation of the Sucher equation, we neglect all spin terms giving us

$$\left[\sqrt{p^2+m_1^2}+\sqrt{p^2+m_2^2}\right]\phi_l(p) + \int_0^\infty A_1(\mathbf{p})A_2(\mathbf{p})V_l(p,p')A_1(\mathbf{p}')A_2(\mathbf{p}')\phi_l(p')p'dp' = E\phi_l(p). \tag{3.20}$$

This equation takes the form of the momentum space Schrödinger equation with relativistic kinematics which is also known as the spinless Salpeter equation with the additional A_i terms. Nonetheless the calculation is very similar to the momentum space Schrödinger equation. We need a meaningful way of comparing to experiment when neglecting spin. One way of comparing to experiment is to use the spin average. The spin average is a weighted average of spin singlet and triplet states. For the spin average, we obtained a weighted average over all of the singlet and triplet states for a given orbital angular momentum. Consider the $l = 0$ state. The singlet state corresponds to $S = 0$ and $J = 0$, and the triplet state for the same orbital angular momentum corresponds to $S = 1$ and $J = 1$. There are $2J + 1$ components of the total angular momentum. The spin averaged mass m_{sa} of the singlet and triplet states for $l = 0$

angular momentum is given by

$$m_{\rm sa} = \frac{m_0^0 + 3m_1^1}{4}, \tag{3.21}$$

where the subscripts indicate J, the superscripts indicate S, and the denominator is the sum of the total number of components. For the $l = 1$ state, the possible values of the total angular momentum is $J = 1$ for the singlet state and $J = 0, 1, 2$ for the triplet state. The weighting factors are determined from the $2J + 1$ components for each J. Thus for the $l = 1$ spin averaged mass, we find

$$m_{\rm sa} = \frac{3m_1^0 + m_0^1 + 3m_1^1 + 5m_2^1}{12} \tag{3.22}$$

and for the $l = 2$ spin averaged mass we find

$$m_{\rm sa} = \frac{5m_2^0 + 3m_1^1 + 5m_2^1 + 7m_3^1}{20}. \tag{3.23}$$

There is a lack of experimental data in which both the singlet states and triplet states are known. Fulcher [36, 37] uses the known triplet states to estimate the singlet states and vice-versa. We will use a similar approach, but the states will be predicted numerically using the mixed-space Schrödinger equation with relativistic kinematics. In addition to using a confining linear and Coulomb-like potential, we use phenomenological potentials for the spin-spin and spin-orbit interaction. One possible phenomenological potential is given by [38]

$$\begin{aligned} V(r) = \sigma r + C/r + V_{SS}[2S(S+1) - 3]e^{-r^2/4{r_0}^2} \\ + \frac{1}{2}V_{LS}\left[J(J+1) - L(L+1) - S(S+1)\right]e^{-\beta r^2}. \end{aligned} \tag{3.24}$$

The first two terms are the usual potentials associated with confinement and asymptotic freedom. The third term includes a parameter for the amplitude V_{SS} and a parameter r_0 for the smeared delta function (approximated as a Gaussian here) associated with the spin-spin interaction. The fourth term is associated with the spin-orbit interaction, where the amplitude is varied with V_{LS} and the singular function form of the potential is approximated with a Gaussian using a parameter β.

In the next section, we will use the mixed space Schrödinger equation with the above potential and fit to available experimental data and then use it to predict unknown singlet and triplet states. Afterwards the weighted averaged of the triplet and singlet states will be obtained. We then fit the spinless Sucher equation (3.20) to the spin averaged data. Finally we implement the Sucher equation with no approximations. We use the potential given in equation (3.18) and fit to low lying triplet states of $c\bar{c}$ and $b\bar{b}$ mesons using the confining coupling constant σ and the Coulomb-like constant C. The remaining spectra is then predicted.

Chapter 4

RESULTS AND CONCLUSIONS

In this section we describe the results for the spinless Sucher equation and the Sucher equation with no approximations. We produce spin average results by using the mixed space Schrödinger equation with relativistic kinematics. We then fit the spinless Sucher equation to the spin averaged results for charmonium and bottomonium. We also present the results for the full Sucher equation with no corrections as it has been used for $c\bar{c}$ and $b\bar{b}$ mass spectra. In our angular momentum analysis of the Sucher equation, we found terms inherently built into the equation that act as spin-spin, spin-orbit (for equal mass cases), and tensor interactions. For the Sucher equation, we have used a simple potential that models confinement and asymptotic freedom, however no phenomenological potentials are used to model spin-spin, spin-orbit, or tensor interactions.

4.1 Spinless Sucher Equation

The spinless mixed space Schrödinger equation with relativistic kinematics, also known as the spinless Salpeter equation, and the spinless Sucher equation (3.20) are solved using the variational principle. Each equation can be written as a matrix eigenvalue equation. The wave function is expanded as a linear combination of orthonormal basis functions formulated from Jacobi polynomials as described in Appendix E. We use 60 basis functions in our computations. The Sucher equation is a relativistic equation which is solved in momentum space. The main difference between the spinless momentum space Schrödinger equation (spinless Salpeter equation) and the spinless Sucher equation with V_0^{eff} is that the effective potential includes the additional relativistic factors of A_i. Although the momentum space spinless Salpeter equation and the spinless Sucher equation are formulated differently, the techniques used to solve these equations are the same.

We used the mixed space Schrödinger equation with relativistic kinematics and potential given by equation (3.24) to fit to the $b\bar{b}$ and $c\bar{c}$ meson systems. We fit to the first two singlet and triplet states of the $b\bar{b}$ system to determine the linear coupling constant σ, the Coulomb-like constant C, and the constituent mass of the bottom quark. In addition the parameters for the spin-spin and spin-orbit interaction was also adjusted to fit to the proper energy level splitting between the triplet and singlet states. Then the remaining $b\bar{b}$ spectrum was predicted. The linear coupling constant and Coulomb-like parameters that were obtained from fitting to the $b\bar{b}$ spectrum were used for all of the remaining mixed spaced calculations. In addition to the

constituent mass m_c of the charmed quark, the parameters associated with the spin-spin and spin-orbit were also varied for the $c\bar{c}$ system to ensure a proper fit. We varied the parameters until we obtained a percent error of less than one percent when compared to experiment.

The results for the mixed-space Schrödinger equation with relativistic kinematics are found in tables 4.1-4.5. We used a linear coupling constant of $\sigma = 0.197$ GeV^2, a Coulomb-like constant of $C = -0.5$, and we used $r_0 = 0.66$ GeV for the spin-spin interaction. We used a constituent quark mass of $m_c = 1.3560$ GeV for the charm quark and $m_b = 4.7839$ GeV for the bottom quark. The parameters used for the fitting procedure are consistent with the literature [39, 36, 40, 41, 37, 42, 43]. The remaining parameters used for the spin-spin and spin-orbit interactions are included in the data tables 4.1-4.5.

Next we obtain a weighted spin average of the singlet and triplet states obtained from the mixed space fit. We then fit the spinless Sucher equation to the spin averaged data by varying the linear coupling constant σ and Coulomb-like constant C. We began by fitting the spinless Sucher equation to the first two spin averaged S states of the $b\bar{b}$ spectra. From this fit we obtained σ, C, and the constituent mass of the bottom quark. Using the same σ and C parameters, we adjusted the constituent mass of the charmed quark to obtain a fit to the first spin averaged $1S$ state of the charmonium system.

The results of fitting the spinless Sucher equation to the spin averaged results are given in tables 4.6 - 4.7. We used a linear coupling constant $\sigma = 0.191$ GeV^2 and a Coulomb constant of $C = -0.555$, and we used a constituent quark mass of $m_c = 1.3587$ GeV for the charm quark and $m_b = 4.7950$ GeV for the bottom quark. We find that the parameters used to obtain the fit for the Sucher equation are consistent with the parameters reported in the literature [39, 36, 40, 41, 37, 42, 43]. Thus we conclude that the Sucher equation may be used for meson spectroscopy. In the next section, we report the results of the full Sucher equation with no approximations when used for $c\bar{c}$ and $b\bar{b}$ mesons.

4.2 Sucher Equation with No Approximations

In this section the Sucher equation is used for $c\bar{c}$ and $b\bar{b}$ mass spectra. The wave function is expanded as a linear combination of orthonormal basis functions formulated from Jacobi polynomials as described in Appendix E. We used 40 basis functions for all of these calculations. The first term of the effective potential V_1^{eff} from equation (2.70) contains no spin, but it does include the relativistic factors A_i. The second two terms V_2^{eff} and V_3^{eff} are related to spin-orbit interaction for equal masses (as is the case for $c\bar{c}$ and $b\bar{b}$ spectra). Each of these two terms is also inversely proportional to square of the mass m^2. The last term V_4^{eff} is related to the spin-spin interaction and the tensor interaction. It is this last term that gives rise to coupling for the $L = J \pm 1$ triplet states. Moreover the fourth term is inversely proportional to m^4. As a result of the proportionality of the mass, one expects to find the most contribution for the V_1^{eff} term and progressively less contribution from V_2^{eff} and V_3^{eff} and finally with the least contribution

coming from V_4^{eff}.

We fit the Sucher equation to the first two $^3S_1$ triplet states of the $b\bar{b}$ system. The linear coupling constant σ and the Coulomb constant C were varied along with constituent mass of the bottom quark until we obtained a fit with a percent error of less than one percent when compared to experiment. Then using the C and σ parameters obtained from the fit to the $b\bar{b}$ system, we varied the charm mass until achieving a fit to the first triplet state of the charmonium spectra. The remaining spectra were then predicted. We used a linear coupling constant of $\sigma = 0.190$ GeV^2 and a Coulomb-like constant of $C = -0.50$. The constituent mass of the charmed quark is $m_c = 1.3438$ GeV and the bottom quark is $m_b = 4.7728$ GeV. The parameters we used here are in agreement with those from the literature [39, 36, 40, 41, 37, 42, 43]. The results for the Sucher equation are found in tables 4.8 - 4.12.

We find that the Sucher equation used with the potential given by equation (3.18) does not produce adequate spin-spin energy level splitting. However the full Sucher equation does produce adequate spin-orbit splitting. The reason for this is that fourth term in the effective potential (2.70) is proportional to the spin-spin and tensor contributions. This term is inversely proportional to m^4, so it will not produce adequate energy level splitting to agree with experiment. The V_2^{eff} and V_3^{eff} terms, which are proportional to the spin-orbit interaction for $c\bar{c}$ and $b\bar{b}$ systems, contribute more to the meson spectroscopy than the fourth term in the effective potential.

We have found that the Sucher equation may be used for $b\bar{b}$ and $c\bar{c}$ spectroscopy. However, the inherent spin dependent terms of the Sucher equation are not adequate to produce spin-spin level splitting. We recommend that phenomenological potentials that include spin-spin interaction be used in the V_1^{eff} term for future studies.

4.3 Conclusions

The Sucher equation has been used for $c\bar{c}$ and $b\bar{b}$ meson spectroscopy. A full angular momentum analysis of the Sucher equation has revealed structure of spin-spin, spin-orbit, and tensor interactions which are inherently built in to the equation. As a first approximation, the spin averaged mass spectra of the $c\bar{c}$ and $b\bar{b}$ meson systems were studied. In addition, the full Sucher equation with no approximations has been used for $c\bar{c}$ and $b\bar{b}$ meson spectra. We have used a linear potential for quark confinement and a Coulomb-like potential to model asymptotic freedom which manifests from the OGE model at short interaction distances. The results confirm that the Sucher equation may be used for $c\bar{c}$ and $b\bar{b}$ mesons. However, the spin-spin interaction inherent to the Sucher equation does not produce adequate energy level splitting between triplet and singlet states. Future studies of the Sucher equation should include additional phenomenological spin-spin terms to produce the energy level splitting between singlet and triplet states. We also note that one needs to take into account the isospin to study other meson systems.

Table 4.1: The Mixed Space Schrödinger Equation has Been Fit to the $b\bar{b}$ Meson System. The Parameters are $m_b = 4.7839$ GeV, $V_{SS} = 0.055$, $V_{LS} = 1.04$, and $\beta = 2.73$ GeV^2

State	Meson	Exp. Val (MeV)	Uncertainty (MeV)	Mixed-Space Fit (MeV)	Per Error (%)
$1\,^1S_0$	$\eta_b(1S)$	9388.9	4.0/-3.5	9389.26	3.9×10^{-3}
$2\,^1S_0$				10022.66	NA
$3\,^1S_0$				10385.86	NA
$4\,^1S_0$				10676.07	NA
$5\,^1S_0$				10928.75	NA
$6\,^1S_0$				11157.38	NA
$1\,^3S_1$	$\Upsilon(1S)$	9460.30	0.26	9460.17	1.4×10^{-3}
$2\,^3S_1$	$\Upsilon(2S)$	10,023.26	0.31	10043.68	0.20
$3\,^3S_1$	$\Upsilon(3S)$	10,355.2	0.5	10399.52	0.43
$4\,^3S_1$	$\Upsilon(4S)$	10,579.4	1.2	10686.74	1.01
$5\,^3S_1$	$\Upsilon(10860)$	10,865	8	10937.75	0.67
$6\,^3S_1$	$\Upsilon(11020)$	11,019	8	11165.28	1.33
$1\,^3P_0$	$\chi_{b0}(1P)$	9859.44	0.73	9859.48	4.1×10^{-4}
$2\,^3P_0$	$\chi_{b0}(2P)$	10,232.5	0.9	10238.14	5.5×10^{-2}
$3\,^3P_0$				10543.19	NA
$4\,^3P_0$				10806.74	NA
$5\,^3P_0$				11043.61	NA
$6\,^3P_0$				11261.52	NA
$1\,^3P_1$	$\chi_{b1}(1P)$	9892.78	0.57	9922.81	0.30
$2\,^3P_1$	$\chi_{b1}(2P)$	10,254.6	0.72	10286.68	0.31
$3\,^3P_1$				10582.14	NA
$4\,^3P_1$				10839.79	NA
$5\,^3P_1$				11072.71	NA
$6\,^3P_1$				11287.79	NA

Table 4.2: The Mixed Space Schrödinger Equation has Been Fit to the $b\bar{b}$ Meson System (Continued). The Parameters are $m_b = 4.7839$ GeV, $V_{SS} = 0.055$, $V_{LS} = 1.04$, and $\beta = 2.73$ GeV^2

State	Meson	Exp. Val (MeV)	Uncertainty (MeV)	Mixed-Space Fit (MeV)	Per Error (%)
$1\,^3P_2$	$\chi_{b2}(1P)$	9912.21	0.57	9980.78	0.69
$2\,^3P_2$	$\chi_{b2}(2P)$	10,268.65	0.72	10343.19	0.73
$3\,^3P_2$				10634.89	NA
$4\,^3P_2$				10889.12	NA
$5\,^3P_2$				11119.12	NA
$6\,^3P_2$				11331.70	NA
$1\,^1P_1$		NA	NA	9931.60	NA
$2\,^1P_1$		NA	NA	10305.28	NA
$3\,^1P_1$		NA	NA	10601.31	NA
$4\,^1P_1$		NA	NA	10858.26	NA
$5\,^1P_1$		NA	NA	11090.26	NA
$6\,^1P_1$		NA	NA	11304.44	NA

Table 4.3: The Mixed Space Schrödinger Equation has Been Fit to the $c\bar{c}$ Meson System. The Parameters are $m_c = 1.356$ GeV, $V_{SS} = 0.179$, $V_{LS} = 2.025$, and $\beta = 1.573$ GeV^2.

State	Meson	Exp. Val (MeV)	Uncertainty (MeV)	Mixed-Space Fit (MeV)	Per Error (%)
1^1S_0	$\eta_c(1S)$	2980.5	1.2	2980.13	1.2×10^{-2}
2^1S_0	$\eta_c(2S)$	3637	4	3637.59	1.6×10^{-2}
3^1S_0				4088.54	NA
4^1S_0				4462.59	NA
5^1S_0				4791.96	NA
6^1S_0				5090.77	NA
1^3S_1	$J/\Psi(1S)$	3096.916	0.011	3096.78	4.3×10^{-3}
2^3S_1	$\Psi(2S)$	3686.09	0.04	3689.00	7.9×10^{-2}
3^3S_1	$\Psi(4040)$	4039	1	4125.36	2.14
4^3S_1	$\Psi(4415)$	4421	4	4492.76	1.62
5^3S_1				4818.15	NA
6^3S_1				5114.24	NA
1^3P_0	$\chi_{c0}(1P)$	3414.75	0.31	3414.53	6.5×10^{-3}
2^3P_0				3835.67	NA
3^3P_0				4219.72	NA
4^3P_0				4565.74	NA
5^3P_0				4879.93	NA
6^3P_0				5168.98	NA
1^3P_1	$\chi_{c1}(1P)$	3510.66	0.07	3499.08	0.33
2^3P_1				3944.46	NA
3^3P_1				4319.61	NA
4^3P_1				4652.90	NA
5^3P_1				4956.72	NA
6^3P_1				5237.96	NA

Table 4.4: The Mixed Space Schrödinger Equation has Been Fit to the $c\bar{c}$ Meson System (Continued). The Parameters are $m_c = 1.356$ GeV, $V_{SS} = 0.179$, $V_{LS} = 2.025$, and $\beta = 1.573$ GeV^2.

State	Meson	Exp. Val (MeV)	Uncertainty (MeV)	Mixed-Space Fit (MeV)	Per Error (%)
1^3P_2	$\chi_{c2}(1P)$	3556.20	0.09	3548.17	0.23
2^3P_2	$\chi_{c2}(2P)$	3929	5	4015.23	2.19
3^3P_2				4400.95	NA
4^3P_2				4738.88	NA
5^3P_2				5044.20	NA
6^3P_2				5325.33	NA
1^1P_1	h_c	3525.67	0.32	3505.14	0.58
2^1P_1				3964.71	NA
3^1P_1				4348.39	NA
4^1P_1				4685.77	NA
5^1P_1				4991.10	NA
6^1P_1				5272.55	NA
1^3D_1	$\Psi(3770)$	3772.92	0.35	3822.06	1.30
2^3D_1	$\Psi(4160)$	4153	3	4203.68	1.22
3^3D_1				4530.12	NA
4^3D_1				4821.97	NA
5^3D_1				5092.73	NA
6^3D_1				5349.72	NA
1^1D_2		NA	NA	3827.29	NA
2^1D_2		NA	NA	4222.50	NA
3^1D_2		NA	NA	4568.21	NA
4^1D_2		NA	NA	4880.25	NA
5^1D_2		NA	NA	5167.31	NA
6^1D_2		NA	NA	5434.83	NA

Table 4.5: The Mixed Space Schrödinger equation has Been Fit to the $c\bar{c}$ Meson System (Continued). The Parameters are $m_c = 1.356$ GeV, $V_{SS} = 0.179$, $V_{LS} = 2.025$, and $\beta = 1.573$ GeV^2.

State	Meson	Exp. Val (MeV)	Uncertainty (MeV)	Mixed-Space Fit (MeV)	Per Error (%)
1^3D_2		NA	NA	3830.40	NA
2^3D_2		NA	NA	4225.99	NA
3^3D_2		NA	NA	4570.32	NA
4^3D_2		NA	NA	4880.19	NA
5^3D_2		NA	NA	5164.87	NA
6^3D_2		NA	NA	5430.08	NA
1^3D_3		NA	NA	3836.36	NA
2^3D_3		NA	NA	4238.91	NA
3^3D_3		NA	NA	4590.13	NA
4^3D_3		NA	NA	4906.36	NA
5^3D_3		NA	NA	5196.71	NA
6^3D_3		NA	NA	5466.88	NA

Table 4.6: The Spinless Sucher Equation has Been Fit to the Spin Averaged Data for $b\bar{b}$ Mesons. The Parameter is $m_b = 4.795$ GeV.

State	Spin Average (MeV)	Sucher Results (MeV)	Percent Error %
1S	9442.44	9441.91	0.01
2S	10038.42	10039.18	0.01
3S	10396.10	10389.24	0.07
4S	10684.08	10667.40	0.16
5S	10935.50	10907.98	0.25
6S	11163.30	11124.32	0.35
1P	9943.88	9934.39	0.10
2P	10310.83	10297.91	0.13
3P	10605.67	10584.20	0.20
4P	10862.21	10830.54	0.29
5P	11094.01	11051.31	0.38
6P	11308.06	11253.82	0.48

Table 4.7: The Spinless Sucher Equation has Been Fit to the Spin Averaged Data for $c\bar{c}$ Mesons. The Parameter is $m_c = 1.3587$ GeV.

State	Spin Average (MeV)	Sucher Results (MeV)	Percent Error %
1S	3067.62	3067.62	0.00
2S	3676.15	3642.82	0.91
3S	4116.15	4038.49	1.89
4S	4485.21	4360.16	2.79
5S	4811.60	4638.09	3.61
6S	5108.38	4886.13	4.35
1P	3514.00	3466.15	1.36
2P	3969.95	3894.28	1.91
3P	4352.37	4234.96	2.70
4P	4689.68	4525.92	3.49
5P	4995.36	4783.66	4.24
6P	5277.26	5017.13	4.93
1D	3830.46	3730.67	2.61
2D	4226.29	4095.20	3.10
3D	4570.70	4401.98	3.69
4D	4880.63	4671.24	4.29
5D	5165.80	4913.61	4.88
6D	5432.09	5135.52	5.46

Table 4.8: The Sucher Equation with No Approximations Fit to $b\bar{b}$ Meson system. Coupled States are Indicated as ${}^3S_1/{}^3D_1$, Where the State in Bold is Dominant. The Constituent Mass of the Bottom Quark is $m_b = 4.7728$ GeV.

State	Meson	Exp. Val (MeV)	Uncertainty (MeV)	Sucher Eq. Fit (MeV)	Per Error (%)
$1\,{}^1S_0$	$\eta_b(1S)$	9388.9	4.0/-3.5	9459.22	0.75
$2\,{}^1S_0$				10,021.34	NA
$3\,{}^1S_0$				10,367.10	NA
$4\,{}^1S_0$				10,646.87	NA
$5\,{}^1S_0$				10,891.62	NA
$6\,{}^1S_0$				11,113.61	NA
$\mathbf{{}^3S_1}/{}^3D_1$	$\Upsilon(1S)$	9460.30	0.26	9460.31	9.5×10^{-5}
$\mathbf{{}^3S_1}/{}^3D_1$	$\Upsilon(2S)$	10,023.26	0.31	10,022.15	1.1×10^{-2}
${}^3S_1\mathbf{{}^3D_1}$				10,146.81	NA
$\mathbf{{}^3S_1}/{}^3D_1$	$\Upsilon(3S)$	10,355.2	0.5	10,367.81	0.12
${}^3S_1\mathbf{{}^3D_1}$				10,453.62	NA
$\mathbf{{}^3S_1}/{}^3D_1$	$\Upsilon(4S)$	10,579.4	1.2	10,647.52	0.64
${}^3S_1\mathbf{{}^3D_1}$				10,708.60	NA
$\mathbf{{}^3S_1}/{}^3D_1$	$\Upsilon(10860)$	10,865	8	10,892.22	0.25
${}^3S_1\mathbf{{}^3D_1}$				10,942.74	NA
$\mathbf{{}^3S_1}/{}^3D_1$	$\Upsilon(11020)$	11,019	8	11,114.17	0.86
${}^3S_1\mathbf{{}^3D_1}$				11,155.11	NA
$1\,{}^3P_0$	$\chi_{b0}(1P)$	9859.44	0.73	9908.06	0.49
$2\,{}^3P_0$	$\chi_{b0}(2P)$	10,232.5	0.9	10,266.05	0.33
$3\,{}^3P_0$				10,554.00	NA
$4\,{}^3P_0$				10,804.47	NA
$5\,{}^3P_0$				11,030.97	NA
$6\,{}^3P_0$				11,240.15	NA

Table 4.9: Sucher Equation with no Approximations Fit to $b\bar{b}$ Meson System (Continued). The Coupled States are Indicated as ${}^3P_2/{}^3F_2$, Where the State in Bold is Dominant. The Constituent Mass of the Bottom Quark is $m_b = 4.7728$ GeV.

State	Meson	Exp. Val (MeV)	Uncertainty (MeV)	Sucher Eq. Fit (MeV)	Per Error (%)
$1\,{}^3P_1$	$\chi_{b1}(1P)$	9892.78	0.57	9911.44	0.19
$2\,{}^3P_1$	$\chi_{b1}(2P)$	10,254.6	0.72	10,269.71	0.15
$3\,{}^3P_1$				10,557.21	NA
$4\,{}^3P_1$				10,807.48	NA
$5\,{}^3P_1$				11,033.75	NA
$6\,{}^3P_1$				11,242.79	NA
$\mathbf{{}^3P_2}/{}^3F_2$	$\chi_{b2}(1P)$	9912.21	0.57	9927.41	0.15
$\mathbf{{}^3P_2}/{}^3F_2$	$\chi_{b2}(2P)$	10,268.65	0.72	10,282.18	0.13
${}^3P_2/\mathbf{{}^3F_2}$				10,313.76	NA
$\mathbf{{}^3P_2}/{}^3F_2$				10,567.99	NA
${}^3P_2/\mathbf{{}^3F_2}$				10,626.62	NA
$\mathbf{{}^3P_2}/{}^3F_2$				10,817.19	NA
${}^3P_2/\mathbf{{}^3F_2}$				10,844.06	NA
$\mathbf{{}^3P_2}/{}^3F_2$				11,042.69	NA
${}^3P_2/\mathbf{{}^3F_2}$				11,081.88	NA
$\mathbf{{}^3P_2}/{}^3F_2$				11,251.11	NA
${}^3P_2/\mathbf{{}^3F_2}$				11,270.92	NA
$1\,{}^1P_1$		NA	NA	9919.58	NA
$2\,{}^1P_1$		NA	NA	10,276.06	NA
$3\,{}^1P_1$		NA	NA	10,562.72	NA
$4\,{}^1P_1$		NA	NA	10,812.48	NA
$5\,{}^1P_1$		NA	NA	11,038.40	NA
$6\,{}^1P_1$		NA	NA	11,247.17	NA

Table 4.10: Sucher Equation with No Approximations Fit to $c\bar{c}$ Meson System. Coupled States are Indicated as ${}^3S_1/{}^3D_1$, where the State in Bold is Dominant. The Constituent Quark mass of the Charmonium is Given by $m_c = 1.3438$ GeV.

State	Meson	Exp. Val (MeV)	Uncertainty (MeV)	Sucher Eq. Fit (MeV)	Per Error (%)
$1\,{}^1S_0$	$\eta_c(1S)$	2980.5	1.2	3095.44	3.86
$2\,{}^1S_0$	$\eta_c(2S)$	3637	4	3667.38	0.84
$3\,{}^1S_0$				4097.97	NA
$4\,{}^1S_0$				4448.54	NA
$5\,{}^1S_0$				4765.75	NA
$6\,{}^1S_0$				5054.72	NA
$\mathbf{{}^3S_1}/{}^3D_1$	$J/\Psi(1S)$	3096.916	0.011	3096.07	2.7×10^{-2}
$\mathbf{{}^3S_1}/{}^3D_1$	$\Psi(2S)$	3686.09	0.04	3668.00	0.49
${}^3S_1/\mathbf{{}^3D_1}$	$\Psi(3770)$	3772.92	0.35	3712.44	1.60
$\mathbf{{}^3S_1}/{}^3D_1$	$\Psi(4040)$	4039	1	4090.97	1.29
${}^3S_1/\mathbf{{}^3D_1}$	$\Psi(4160)$	4153	3	4138.14	0.36
$\mathbf{{}^3S_1}/{}^3D_1$	$\Psi(4415)$	4421	4	4447.73	0.6
${}^3S_1/\mathbf{{}^3D_1}$				4477.59	NA
$\mathbf{{}^3S_1}/{}^3D_1$				4764.26	NA
${}^3S_1/\mathbf{{}^3D_1}$				4795.25	NA
$\mathbf{{}^3S_1}/{}^3D_1$				5052.56	NA
${}^3S_1/\mathbf{{}^3D_1}$				5345.78	NA
$1\,{}^3P_0$	$\chi_{c0}(1P)$	3414.75	0.31	3493.23	2.3
$2\,{}^3P_0$				3953.26	NA
$3\,{}^3P_0$				4335.51	NA
$4\,{}^3P_0$				4669.42	NA
$5\,{}^3P_0$				4791.27	NA
$6\,{}^3P_0$				5248.91	NA

Table 4.11: Sucher Equation with No Approximations Fit to $c\bar{c}$ Meson System (Continued). Coupled States are Indicated as ${}^3P_2/{}^3F_2$, where the State in Bold is Dominant. The Constituent Quark Mass of Charmed Quark is $m_c = 1.3438$ GeV.

State	Meson	Exp. Val (MeV)	Uncertainty (MeV)	Sucher Eq. Fit (MeV)	Per Error (%)
$1\,{}^3P_1$	$\chi_{c1}(1P)$	3510.66	0.07	3467.66	1.55
$2\,{}^3P_1$				3921.00	NA
$3\,{}^3P_1$				4296.85	NA
$4\,{}^3P_1$				4626.95	NA
$5\,{}^3P_1$				4925.72	NA
$6\,{}^3P_1$				5201.18	NA
$\mathbf{{}^3P_2}/{}^3F_2$	$\chi_{c2}(1P)$	3556.20	0.09	3514.47	1.17
${}^3P_2/\mathbf{{}^3F_2}$				3747.39	NA
$\mathbf{{}^3P_2}/{}^3F_2$	$\chi_{c2}(2P)$	3929	5	3952.93	0.61
$\mathbf{{}^3P_2}/{}^3F_2$				4319.93	NA
${}^3P_2/\mathbf{{}^3F_2}$				4368.57	NA
$\mathbf{{}^3P_2}/{}^3F_2$				4615.39	NA
${}^3P_2/\mathbf{{}^3F_2}$				4644.37	NA
$\mathbf{{}^3P_2}/{}^3F_2$				4938.06	NA
${}^3P_2/\mathbf{{}^3F_2}$				4980.21	NA
${}^3P_2/\mathbf{{}^3F_2}$				5201.86	NA
$\mathbf{{}^3P_2}\,{}^3F_2$				5211.45	NA
$1\,{}^1P_1$	h_c	3525.67	0.32	3493.64	0.91
$2\,{}^1P_1$				3940.34	NA
$3\,{}^1P_1$				4312.72	NA
$4\,{}^1P_1$				4640.63	NA
$5\,{}^1P_1$				4937.85	NA
$6\,{}^1P_1$				5212.15	NA

Table 4.12: Sucher Equation with No Approximations Fit to $c\bar{c}$ Meson System (Continued). The Constituent Mass of the Charmed Quark is $m_c = 1.3438$ GeV.

State	Meson	Exp. Val (MeV)	Uncertainty (MeV)	Sucher Eq. Fit (MeV)	Per Error (%)
$1\,^1D_2$		NA	NA	3806.40	NA
$2\,^1D_2$		NA	NA	4199.07	NA
$3\,^1D_2$		NA	NA	4536.49	NA
$4\,^1D_2$		NA	NA	4843.82	NA
$5\,^1D_2$		NA	NA	5124.12	NA
$6\,^1D_2$		NA	NA	5386.91	NA
$1\,^3D_2$		NA	NA	3797.72	NA
$2\,^3D_2$		NA	NA	4193.24	NA
$3\,^3D_2$		NA	NA	4532.35	NA
$4\,^3D_2$		NA	NA	4840.90	NA
$5\,^3D_2$		NA	NA	5122.06	NA
$6\,^3D_2$		NA	NA	5385.54	NA

Appendix A

VARIATIONAL PRINCIPLE

In this section, the variational principle will be derived [22]. Suppose we operate with a Hamiltonian on a trial wave function $|\psi\rangle$

$$H|\psi\rangle = \tilde{E}|\psi\rangle \tag{A.1}$$

where $\tilde{E}$ is the energy. Now we will expand the wave function in terms of a complete orthonormal set of basis vectors

$$|\psi\rangle = \sum_j c_j|\xi_j\rangle. \tag{A.2}$$

where $|\xi_j\rangle$ are eigenstates of the Hamiltonian: $H|\xi_\mathbf{j}\rangle = E_j|\xi_\mathbf{j}\rangle$ If we project with $\langle\psi|$ onto the left of equation (A.1) and use the the expansion above, then we have

$$\sum_{ij} E_j\langle\xi_i|\xi_j\rangle c_i^* c_j = \tilde{E}\sum_{ij}\langle\xi_i|\xi_j\rangle c_i^* c_j \tag{A.3}$$

Now using using the orthogonality condition $\langle\xi_i|\xi_j\rangle = \delta_{ij}$, the above equation becomes

$$\sum_j E_j c_j^* c_j = \tilde{E} \tag{A.4}$$

Now if we replace E_j with E_0 then we obtain the following inequality

$$E_0\sum_j |c_j|^2 = E_0 \leq \tilde{E} \tag{A.5}$$

We have shown that the energy must be at least equal to the ground state energy.

Next we consider the Schrödinger equation

$$H|\phi\rangle = E|\phi\rangle \tag{A.6}$$

where $|\phi\rangle$ is the exact wave function solution of the Schrödinger equation and E is the energy. We expand the wave function in a complete set of basis vectors,

$$|\phi\rangle = \sum_j c_j|\eta_j\rangle \tag{A.7}$$

with orthonormality condition $\langle\eta_i|\eta_j\rangle = \delta_{ij}$. Note that in this case, $|\eta_j\rangle$ are not eigenstates of the Hamiltonian. Now we project with $\langle\phi|$ onto equation (A.6) and use the expansion above

$$\sum_{ij}\langle\eta_i|H|\eta_j\rangle c_i^* c_j = E\sum_{ij}\langle\eta_i|\eta_j\rangle c_i^* c_j \tag{A.8}$$

Using the orthonormality condition and defining $H_{ij} = \langle \eta_i | H | \eta_j \rangle$ gives us

$$\sum_{ij} H_{ij} c_i^* c_j = E \sum_j c_j^* c_j \tag{A.9}$$

Now we vary the above equation with respect to the coefficients c_k^*,

$$\sum ij H_{kj} c_j = \frac{\partial E}{\partial c_k^*} \sum_j c_i^* c_j + E c_k \tag{A.10}$$

Next we minimize the energy with respect to the coefficients

$$\frac{\partial E}{\partial c_k^*} = 0 \tag{A.11}$$

and this gives us

$$\sum_j H_{kj} c_j = E c_k \tag{A.12}$$

which we may represent as an infinite dimensional matrix

$$\begin{pmatrix} H_{11} & H_{12} & H_{13} & \dots \\ H_{21} & H_{22} & H_{23} & \dots \\ H_{31} & H_{32} & H_{33} & \dots \\ \vdots & \vdots & \vdots & \ddots \end{pmatrix} \begin{pmatrix} c_1 \\ c_2 \\ c3 \\ \vdots \end{pmatrix} = E \begin{pmatrix} c_1 \\ c_2 \\ c3 \\ \vdots \end{pmatrix} \tag{A.13}$$

In practice, one cannot use an infinite number of basis functions in the basis set. Instead, the wave function is expanded in a large but finite number $N_{\max}$ of basis vectors

$$|\phi\rangle = \sum_{j=1}^{N_{\max}} |\eta_j\rangle. \tag{A.14}$$

At this stage the energy is no longer exactly E but is some other energy $\tilde{E}$. Therefore we will use the principle that we derived in equation A.5 and equation A.12 becomes

$$\sum_{j=1}^{N_{\max}} H_{kj} c_j \geq E_0 c_k \tag{A.15}$$

In order to approach the upper bound of the ground state energy, E_0, we will use wave function with a variational parameter. The variational parameter in the wave function is used to compensate for the truncation of the complete set of basis functions.

Appendix B

ENERGY PROJECTORS

In this section, we will briefly discuss the positive and negative energy projectors. Consider the Dirac equation with no interaction where $\hbar = c = 1$,

$$(\not{p} - m)\psi = 0 \tag{B.1}$$

which has plane wave solutions of the form

$$\psi(x) = Ne^{-ix\cdot p}u(p) \tag{B.2}$$

where $x \cdot p = x_\mu p^\mu$ is the four vector scalar product. Note that ψ is a column vector with four elements. Therefore $u(p)$ will consist of four elements. Using this solution, we find

$$(\not{p} - m)u(p) = 0 \tag{B.3}$$

which in matrix form is given by

$$\begin{pmatrix} E-m & \mathbf{p}\cdot\boldsymbol{\sigma} \\ \mathbf{p}\cdot\boldsymbol{\sigma} & -E-m \end{pmatrix}\begin{pmatrix} u_A \\ u_B \end{pmatrix} = 0 \tag{B.4}$$

where we have used u_A to represent the upper two components of u and u_B to represent the lower two components of u. The solution is trivial unless the determinant of the above matrix is zero. After taking the determinant, we find two energy solutions

$$E = \pm\sqrt{p^2+m^2} = \pm|E| \tag{B.5}$$

and we find [18]

$$u_A = \frac{\mathbf{p}\cdot\boldsymbol{\sigma}}{E-m}u_B \qquad u_B = \frac{\mathbf{p}\cdot\boldsymbol{\sigma}}{E+m}u_A \tag{B.6}$$

We associate u_B with the positive energies where $E = |E|$ and u_A with the negative energies where $E = -|E|$, thus

$$u_A = \frac{-\mathbf{p}\cdot\boldsymbol{\sigma}}{|E|+m}u_B \qquad u_B = \frac{\mathbf{p}\cdot\boldsymbol{\sigma}}{|E|+m}u_A. \tag{B.7}$$

In addition, we use the normalization that $u^\dagger u = 2|E|$. Any state may be expanded in a linear combination of the positive and negative energy spinors [44]

$$\psi = \sum_s c_- u_A^s + \sum_s c_+ u_B^s \tag{B.8}$$

where we have summed over the possible spins and c_- and c_+ are the coefficients. We will be interested in projecting out the positive or negative energy states of the state ψ. The positive and negative energies as defined by Sucher are

$$\lambda_\pm = \frac{E \pm (\mathbf{p}\cdot\boldsymbol{\alpha} + \beta m)}{2E}. \tag{B.9}$$

which in matrix form is represented as

$$\lambda_\pm = \frac{1}{2E}\begin{pmatrix} E \pm m & \pm\mathbf{p}\cdot\boldsymbol{\sigma} \\ \pm\mathbf{p}\cdot\boldsymbol{\sigma} & E \mp m \end{pmatrix} \tag{B.10}$$

The positive energy projectors operate according to

$$\lambda_+ u_A = 0 \qquad \lambda_+ u_B = u_B \tag{B.11}$$

and the negative energy projectors operate according to

$$\lambda_- u_A = u_A \qquad \lambda_- u_B = 0 \tag{B.12}$$

Thus the positive and negative operators will separate out the positive and negative energy parts

$$\lambda_+\psi = \sum_s c_- u_A^s \quad \text{and} \quad \lambda_-\psi = \sum_s c_+ u_B^s. \tag{B.13}$$

Appendix C

RACAH AND CLEBSCH-GORDAN COEFFICIENTS

In this section we briefly comment on the the Racah and Clebsch-Gordan coefficients. The phase factors we have used are described by Rotenberg [23]. The 3j symbols are related to the Clebsch-Gordan Coefficients by

$$\begin{pmatrix} j_1 & j_2 & j_3 \\ m_1 & m_2 & m_3 \end{pmatrix} = \frac{(-1)^{j_1-j_2-m_3}}{\sqrt{2j_3+1}}(j_1\, m_1\, j_2\, m_2|j_1\, j_2\, j_3\, -m_3) \tag{C.1}$$

where the 3j symbols are on the left and the Clebsch-Gordan coefficients are on the right.

The 6j symbols are related to the Racah coefficients by

$$\begin{Bmatrix} j_1 & j_2 & j_3 \\ l_1 & l_2 & l_3 \end{Bmatrix} = (-1)^{j_1+j_2+l_1+l_2} W(j_1\, j_2\, l_2\, l_1; j_3 l_3) \tag{C.2}$$

where the 6j symbols are indicated on the left side of the equal sign and the Racah coefficients are indicated on the right. General expressions for computation of the 3j and 6j symbols have been worked out by Rotenberg [23].

Appendix D

GAUSSIAN QUADRATURE

This discussion on Gaussian quadrature is taken from Werneth et. al. [45].. We use Gaussian Quadrature to evaluate an integral using the following approximation [1]:

$$\int_{-1}^{1} f(x)dx \approx \sum_{i=0}^{n-1} w_i f(x_i), \tag{D.1}$$

where f is the function, x_i are the roots of the Legendre polynomials, n is the number of Gaussian points to be used for the summation in equation (D.1). The weights w_i are determined from the derivatives of the Legendre Polynomials evaluated at x_i. The weights used in equation (D.1) are given by

$$w_i = \frac{2}{(1-x_i^2)[P_l'(x_i)]^2}, \tag{D.2}$$

where $P_l'(x_i)$ are the derivatives of the Legendre Polynomials evaluated at x_i.

We usually transform the integrals such that we can use equation (D.1). We transform the integral by using a substitution of the variable. Suppose we were interested in evaluating $\int_0^\infty f(x')dx'$. We can transform the above integral into an integral suitable for Gaussian integration by using the following substitution of variable,

$$x' = \tan\left[\frac{\pi}{4}(x+1)\right]. \tag{D.3}$$

If we use the substitution in equation (D.3) ,then $x' \to 0$ as $x \to -1$ and $x' \to \infty$ as $x \to -1$, giving us

$$\begin{aligned} \int_0^\infty f(x')dx' &= \int_{-1}^{1} f\left\{\tan\left[\frac{\pi}{4}(x+1)\right]\right\} \frac{\pi}{4}\sec^2\left[\frac{\pi}{4}(x+1)\right]dx \\ &\approx \sum_{i=0}^{n-1} f\left\{\tan\left[\frac{\pi}{4}(x_i+1)\right]\right\} \frac{\pi}{4} w_i \sec^2\left[\frac{\pi}{4}(x_i+1)\right]. \end{aligned} \tag{D.4}$$

Now that the variable has been transformed into equation of form (D.1, we can carry out the summation to compute the integral.

Appendix E

BASIS FUNCTIONS

In this Appendix we list the orthonormal basis functions that are used in this dissertation. The basis functions are described by Polyzou and Keister [38]. For position space wave functions we use the following Laguerre basis

$$g_j(r) = \frac{(br)^{l+1}}{b\sqrt{N_j^L}} L_j^{2l+2}(2br)e^{-br}, \tag{E.1}$$

where $L_\alpha^\beta(x)$ are the Laguerre polynomials and the normalization is given by

$$N_j^L \equiv b^{-3}\left(\frac{1}{2}\right)^{2l+3}\frac{\Gamma(j+2l+3)}{j!}. \tag{E.2}$$

The variational parameter is b and $i = 0,1,2,\ldots$ are the indices. The position space basis function satisfies the orthonormality condition

$$\int_0^\infty g_i(r)g_j(r)r^2dr = \delta_{ij}. \tag{E.3}$$

As for the momentum space basis, we use the Bessel Fourier transform of the Laguerre basis given by (cite Polyzou and Keister)

$$\tilde{g}_j(p) = \frac{1}{\sqrt{N_j^J}}\frac{(p/b)^l}{[(p/b)^2+1]^{l+2}}P_i^{(l+3/2,l+1/2)}\left(\frac{p^2-b^2}{p^2+b^2}\right) \tag{E.4}$$

where $P_i^{(l+3/2,l+1/2)}$ are the Jacobi polynomials and the normalization is given by

$$N_j^J = \frac{b^3}{2(2i+2l+3)}\frac{\Gamma(j+l+5/2)\Gamma(j+l+3/2)}{j!\,\Gamma(j+2l+3)} \tag{E.5}$$

The momentum space basis function satisfies the orthonormality condition

$$\int_0^\infty \tilde{g}_i(p)\tilde{g}_j(p)p^2dp = \delta_{ij}. \tag{E.6}$$

Appendix F

MOMENTUM-SPACE POTENTIALS

This appendix highlights the main results on the treatment of Coulomb-like and linear potentials from Maung et. al. [46]. The momentum space Schrödinger equation is written

$$T(\mathbf{p})\phi(\mathbf{p}) + \int V(\mathbf{q})\phi(\mathbf{p}')d\mathbf{p}' = E\phi(\mathbf{p}). \tag{F.1}$$

where $T(\mathbf{p})$ is the kinetic energy operator. If we assume the following form of the potential $V(r) = \lambda_N r^N e^{-\eta r}$ then the Fourier transform of this is given by

$$V(\mathbf{q}) = \frac{\lambda_N}{2\pi^2} \lim_{\eta\to 0}(-1)^{N+1} \frac{\partial^{N+1}}{\partial \eta^{N+1}} \left[\frac{1}{q^2+\eta^2}\right] \tag{F.2}$$

By decomposing the wave function and expanding the potential in spherical harmonics, we can show that the lth partial wave of the momentum space Schrödinger equation is given by

$$T(p)\phi_l(p) + \int_0^\infty V_l(p,p')\phi_l(p')p'^2 dp' = E\phi_l(p') \tag{F.3}$$

The lth partial wave is related to the Fourier transform of the position space potential by

$$V_l(p,p') = 2\pi \int_{-1}^{1} V(\mathbf{q})P_l(x)dx \tag{F.4}$$

where x is defined as $cos(\theta_{pp'})$ and $\theta_{pp'}$ is the angle between $\mathbf{p}$ and $\mathbf{p}'$. Maung et. al. [46] showed that the lth partial wave could be expressed in terms of Legendre polynomials of the second kind $Q_L(y)$

$$y = \frac{p^2 + p'^2 + \eta^2}{2pp'} \tag{F.5}$$

The lth partial wave is given as

$$V_l(p,p') = \lim_{\eta\to 0}(-1)^{N+1} \frac{\partial^{N+1}}{\partial \eta^{N+1}} \frac{Q_l(y)}{pp'} \tag{F.6}$$

For the Coulomb-like potential we take $N = -1$ and for the linear potential we take $N = 1$. The Coulomb-like potential is given by

$$V_l(p,p') = \frac{\lambda_c}{\pi} \lim_{\eta\to 0} \frac{Q_l(y)}{pp'} \tag{F.7}$$

and the linear potential is given in terms of derivatives of the Legendre polynomials of the second kind

$$V_l(p,p') = \frac{\lambda_L}{\pi} \lim_{\eta\to 0} \left[\frac{Q_l'(y)}{(pp')^2} + \frac{\eta^2}{(pp')^3} Q_l''(y)\right] \tag{F.8}$$

where the primes indicate derivatives with respect to the y variable. Maung [46] showed that if one uses an even number Gaussian quadrature points and uses the subtraction methods listed below, then the singularities are overcome. The result of using the subtraction method with $\eta \to 0$ for the linear potential is

$$T(p)\phi_l(p) + \frac{\lambda_C}{\pi p}\int_0^\infty \frac{P_l(y)Q_0(y)}{p'}\left[p'^2\phi_l(p') - \frac{p^2\phi_l(p)}{P_l(y)}\right]dp' \tag{F.9}$$
$$+\frac{\lambda_C}{\pi p}\left[\frac{\pi^2}{2}p^2\phi_l(p)\right] - \frac{\lambda_C}{\pi p}\int_0^\infty w_{l-1}(y)\phi_l(p')p'dp' = E\phi_l(p)$$

where $P_l(y)$ are the Legendre polynomials and

$$w_{l-1}(y) = \sum_{m=1}^{l}\frac{1}{m}P_{l-m}(y)P_{m-1}(y). \tag{F.10}$$

The result of using the subtraction method with $\eta \to 0$ for the coulomb-like potential is given by

$$T(p)\phi_l(p) + \frac{\lambda_L}{\pi p^2}\int_0^\infty P_l(y)Q_0'(y)\left[\phi_l(p') - \frac{\phi_l(p)}{P_l(y)}\right]dp' \tag{F.11}$$
$$+\frac{\lambda_L}{\pi p^2}\int_0^\infty P_l'(y)\frac{Q_0(y)}{p'}\left[p'\phi_l(p') - \frac{l(l+1)}{2}\frac{p\phi_l(p)}{P_l'(y)}\right]dp'$$
$$+\frac{\lambda_L}{\pi p^2}\frac{l(l+1)}{2}\left[\frac{\pi^2}{2}p\phi_l(p)\right] - \frac{\lambda_L}{\pi p^2}\int_0^\infty w_{l-1}'(y)\phi_l(p')dp' = E\phi_l(p)$$

The results listed in equations (F.9) and (F.11) were used extensively for all calculations in momentum space.

BIBLIOGRAPHY

[1] M. Abramowitz and I. A. Stegun. *Handbook of Mathematical Functions*. Dover, 1970.

[2] A. G. Van Melson. *From Atomos to Atom: The History of the Concept Atom*. Duquense University Press, 1952.

[3] F. Leone. *The Atom*. Helix Press, 1986.

[4] M. R. Wehr and J. A. Richards. *Physics of the Atom*. Addison-Wesley Publishing Company, 1967.

[5] H. Semat and H. E. White. *Atomic Age Physics*. Rinehart & Company, Inc., 1959.

[6] P. A. Tipler. *Modern Physics*. Worth Publishers, 1978.

[7] A. T. Goble and D. K. Baker. *Elements of Modern Physics*. The Ronald Press Company, 1971.

[8] D. Griffiths. *Introduction to Quantum Mechanics*. Prentice Hall, Inc., 1987.

[9] P. C. W. Davies. *The forces of nature*. Cambridge University Press, 1986.

[10] G. Fraser. *The particle century*. IOP Publishing IOP Ltd, 1998.

[11] R. S. Skankland. Michelson-morley experiment. *Americal Journal of Physics*, 32:16, 1964.

[12] G. Saathoff et. al. Experimental tests of time dilation in special relativity. *Phys. Rev. Lett.*, 91(190403), 2003.

[13] H.E. Ives and G.R. Stillwell. An experimental study of the rate of a moving clock. *J. Opt. Soc. Am.*, 28:215, 1938.

[14] E. S. Abers. *Quantum Mechanics*. Pearson Education, Inc., 2004.

[15] H. C. Ohanian. *Quantum Mechanics*. Pearson Education, Inc., 2004.

[16] F. Mandl and G. Shaw. *Quantum Field Theory*. John Wiley & Sons, 1984.

[17] W. Greiner and J. Reinhardt. *Field Quantization*. Spinger, 1996.

[18] D. Griffiths. *Introduction to Elementary Particles*. John Wiley & Sons, 1987.

[19] G. E. Brown and D. G. Ravenhall. *Proc. Roy. Soc. Ser. A*, 208(552), 1951.

[20] J. D. Jackson. *Classical Electrodynamics*. John Wiley & Sons, Inc., 1999.

[21] J. Sucher and G. Hardekopf. *Phys. Rev. A*, 30(703), 1984.

[22] M. Weissbluth. *Atoms and Molecules*. Academic Press, 1978.

[23] M. Rotenberg, R. Bivens, N. Metropolis, and J. K. Wooten. *The 3j and 6j symbols*. MIT Press, 1959.

[24] A. Messiah. *Quantum Mechanics*. Dover, 1999.

[25] T. Kopaleishvilli. *Bound $q\bar{q}$ systems in the framework of different versions of 3D reductions of the Bethe-Salpeter equation.* PhD thesis, Tbilisi State University, 2008.

[26] M. Alonso and H. Valk. *Quantum Mechanics: Principles and Applications*. Addison-Wesley Educational Publishers Inc., 1974.

[27] W. Lucha, F. F. Schöberl, and D. Gromes. *Phys. Rep.*, 200(127), 1991.

[28] T. Sato and T. S. H. Lee. *J. Phys. G: Nucl. Part. Phys.*, 36(073001), 2009.

[29] M. M. Giannini, E. Santopinto, and A. Vassalo. *Prog. Part. Nucl. Phys.*, 50(263), 2003.

[30] E. S. Swanson. *Phys. Rep.*, 429(243), 1986.

[31] R. R. Horgan et al. *Phys. Rev. D*, 80(074505), 2009.

[32] P. M. Lo and E. S. Swanson. *Phys. Rev. D*, 81(034030), 2010.

[33] R. Gilman and F. Gross. *J. Phys. G: Nucl. Part. Phys.*, 28(R37), 2002.

[34] R. Machleidt, K. Hilnde, and C. Elster. *Phys. Rep*, 134(1), 1987.

[35] C. M. Werneth, M. Dhar, K. Maung, J. W. Norbury, and C. Sirola. *J. Phys. A: Math. Theo.*, 43(255306), 2010.

[36] L. P. Fulcher, Z. Chen, and K. C. Yeong. *Phys. Rev. D*, 47(4122), 1993.

[37] L. P. Fulcher. *Phys. Rev. D*, 50(447), 1994.

[38] B. D. Polyzou and W. N Keister. Useful bases for problems in nuclear and particle physics. *J. Comp. Phys.*, 47(4122), 1997.

[39] A. Barchielli, N. Brambilla, and G. M. Prosperi. *Il Nuovo Cimento*, 103(59), 1990.

[40] L. P. Fulcher. *Phys. Rev. D*, 34(2857), 1986.

[41] L. P. Fulcher. *Phys. Rev. D*, 37(1258), 1988.

[42] S. Godfrey and N. Isgur. *Phys. Rev. D*, 32(189), 1985.

[43] H. Hersbach. *Phys. Rev. D*, 50(2562), 1994.

[44] F. Gross. *Relativistic Quantum Mechanics and Field Theory*. John Wiley & Sons, Inc., 1993.

[45] C. M. Werneth, M. Dhar, K. Maung, J. W. Norbury, and C. Sirola. *Eur. J. Phys.*, 31(693), 2009.

[46] K. M. Maung, D. E. Kahana, and J. W. Norbury. *Phys. Rev. D*, 47(1182), 1993.